Chapter 10: Mantle Melting and the Generation of Basaltic Magma

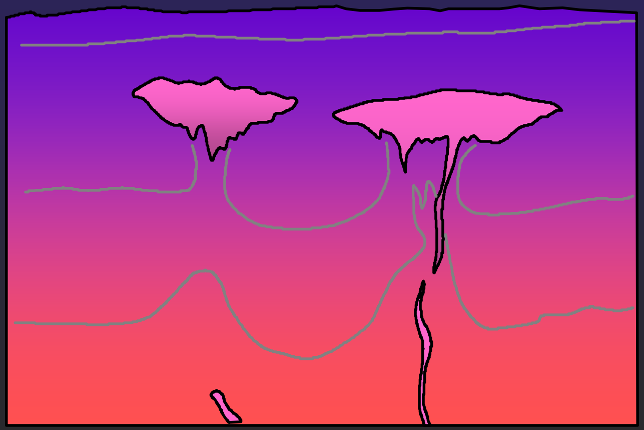

2 principal types of basalt in the ocean basins

Tholeiitic Basalt and *Alkaline* Basalt

Table 10.1 Common petrographic differences between tholeiitic and alkaline basalts

	Tholeiitic Basalt	Alkaline Basalt
Groundmass	Usually fine-grained, intergranular	Usually fairly coarse, intergranular to ophitic
	No olivine	Olivine common
	Clinopyroxene = augite (plus possibly pigeonite)	Titaniferous augite (reddish)
	Orthopyroxene (hypersthene) common, may rim ol.	Orthopyroxene absent
	No alkali feldspar	Interstitial alkali feldspar or feldspathoid may occur
	Interstitial glass and/or quartz common	Interstitial glass rare, and quartz absent
Phenocrysts	Olivine rare, unzoned, and may be partially resorbed or show reaction rims of orthopyroxene	Olivine common and zoned
	Orthopyroxene uncommon	Orthopyroxene absent
	Early plagioclase common	Plagioclase less common, and later in sequence
	Clinopyroxene is pale brown augite	Clinopyroxene is titaniferous augite, reddish rims

after Hughes (1982) and McBirney (1993).

Each is chemically distinct

Evolve via FX as separate series along different paths

- Tholeiites are generated at mid-ocean ridges
  - Also generated at oceanic islands, subduction zones
- Alkaline basalts generated at ocean islands
  - Also at subduction zones

Sources of mantle material

- ***Ophiolites***
  - ☞ Slabs of oceanic crust and upper mantle
  - ☞ Thrust at subduction zones onto edge of continent
- ***Dredge samples*** from oceanic crust
- ***Nodules*** and ***xenoliths*** in some basalts
- ***Kimberlite xenoliths***
  - ☞ Diamond-bearing pipes blasted up from the mantle carrying numerous xenoliths from depth

Lherzolite is probably fertile unaltered mantle

Dunite and harzburgite are refractory residuum after basalt has been extracted by partial melting

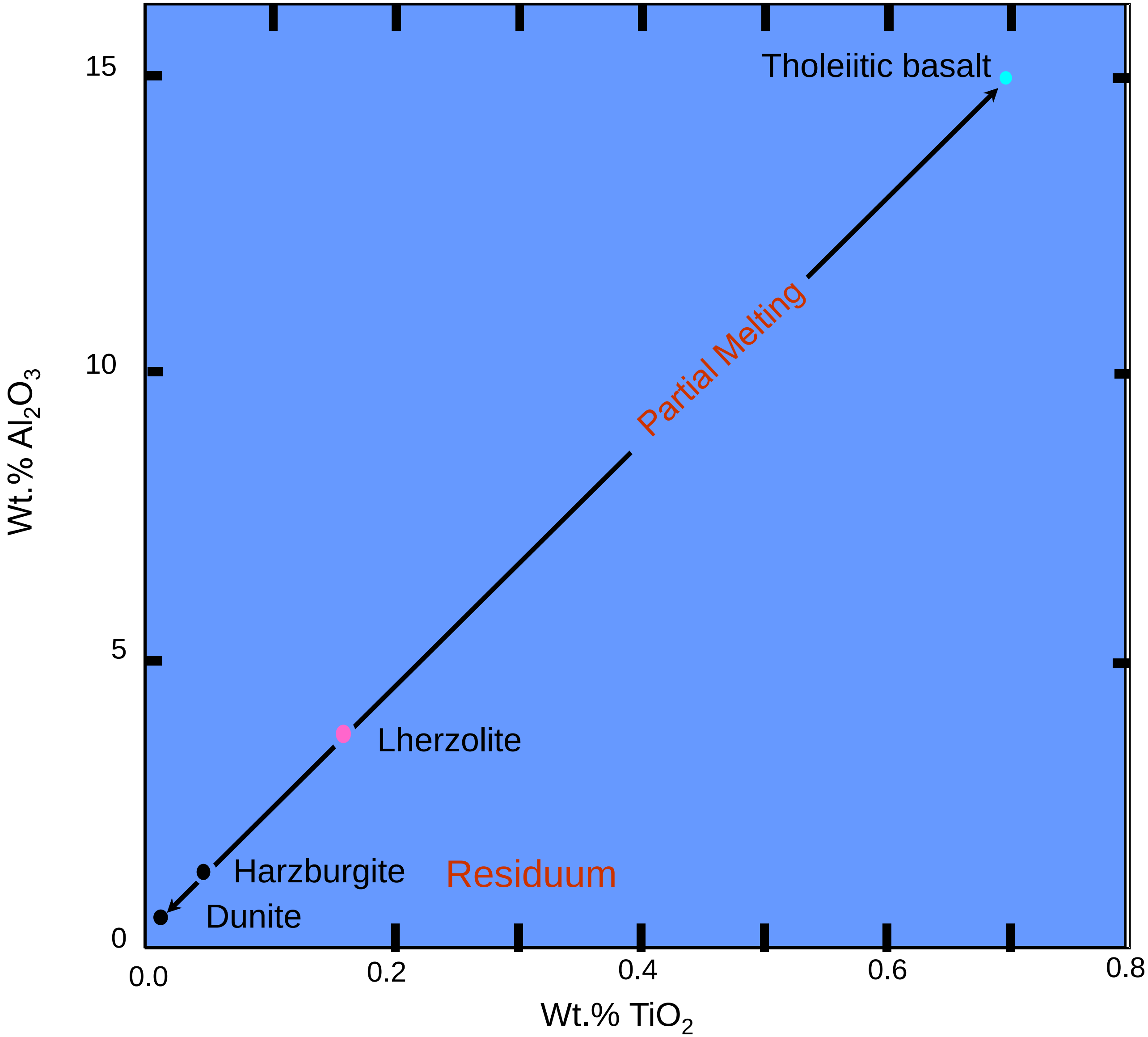

Figure 10-1 **Brown and Mussett, A. E. (1993),** ***The Inaccessible Earth: An Integrated View of Its Structure and Composition.*** **Chapman & Hall/Kluwer.**

Lherzolite: A type of peridotite with Olivine > Opx + Cpx

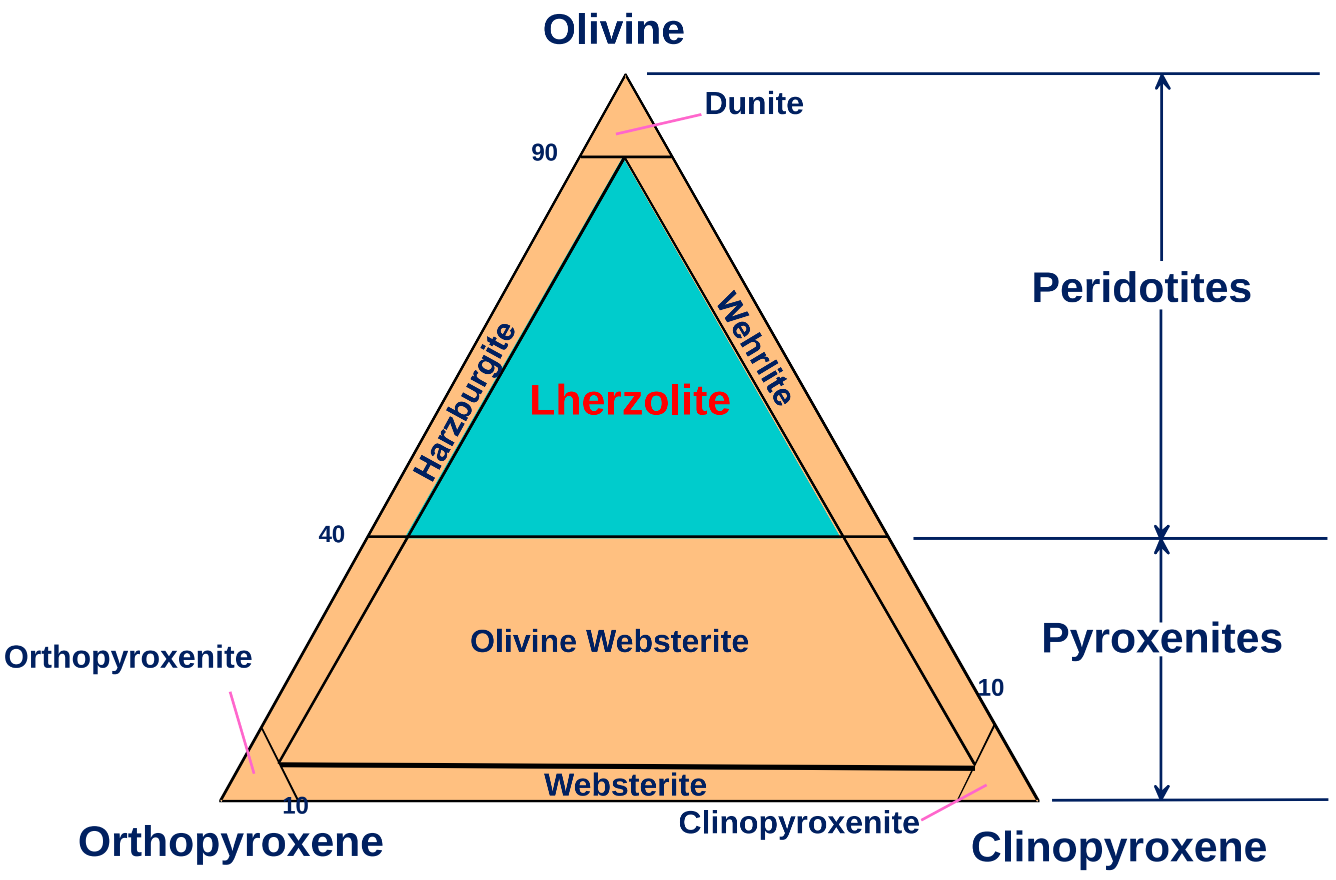

Figure 2.2 C After IUGS

Phase diagram for aluminous 4-phase lherzolite:

Al-phase =

- Plagioclase
  - shallow (< 50 km)
- Spinel
  - 50-80 km
- Garnet
  - 80-400 km
- Si → VI coord.
  - > 400 km

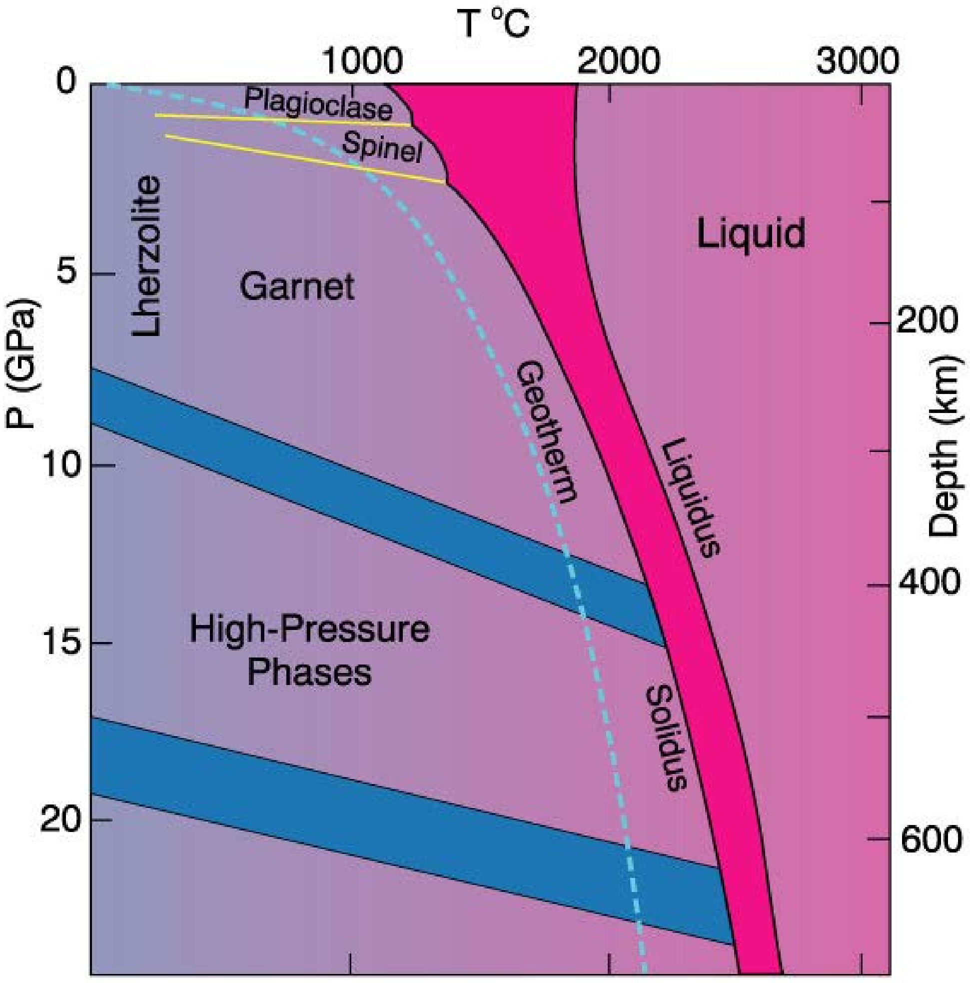

Figure 10.2 Phase diagram of aluminous lherzolite with melting interval (gray), sub-solidus reactions, and geothermal gradient. After Wyllie, P. J. (1981). Geol. Rundsch. 70, 128-153.

How does the mantle melt??

1) Increase the temperature

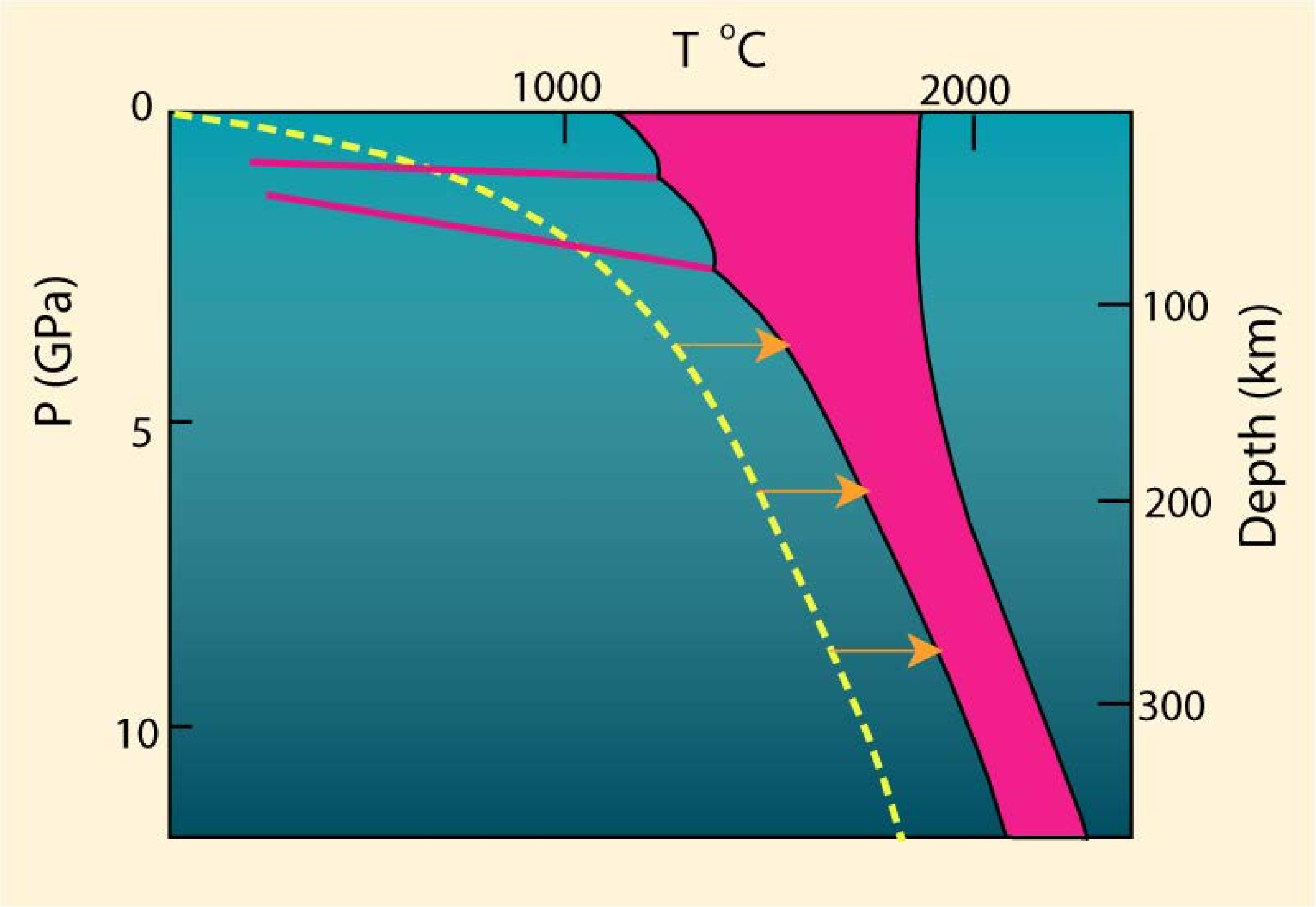

Figure 10.3. Melting by raising the temperature.

2) Lower the pressure

- *Adiabatic* rise of mantle with no conductive heat loss
- *Decompression partial melting* could melt at least 30%

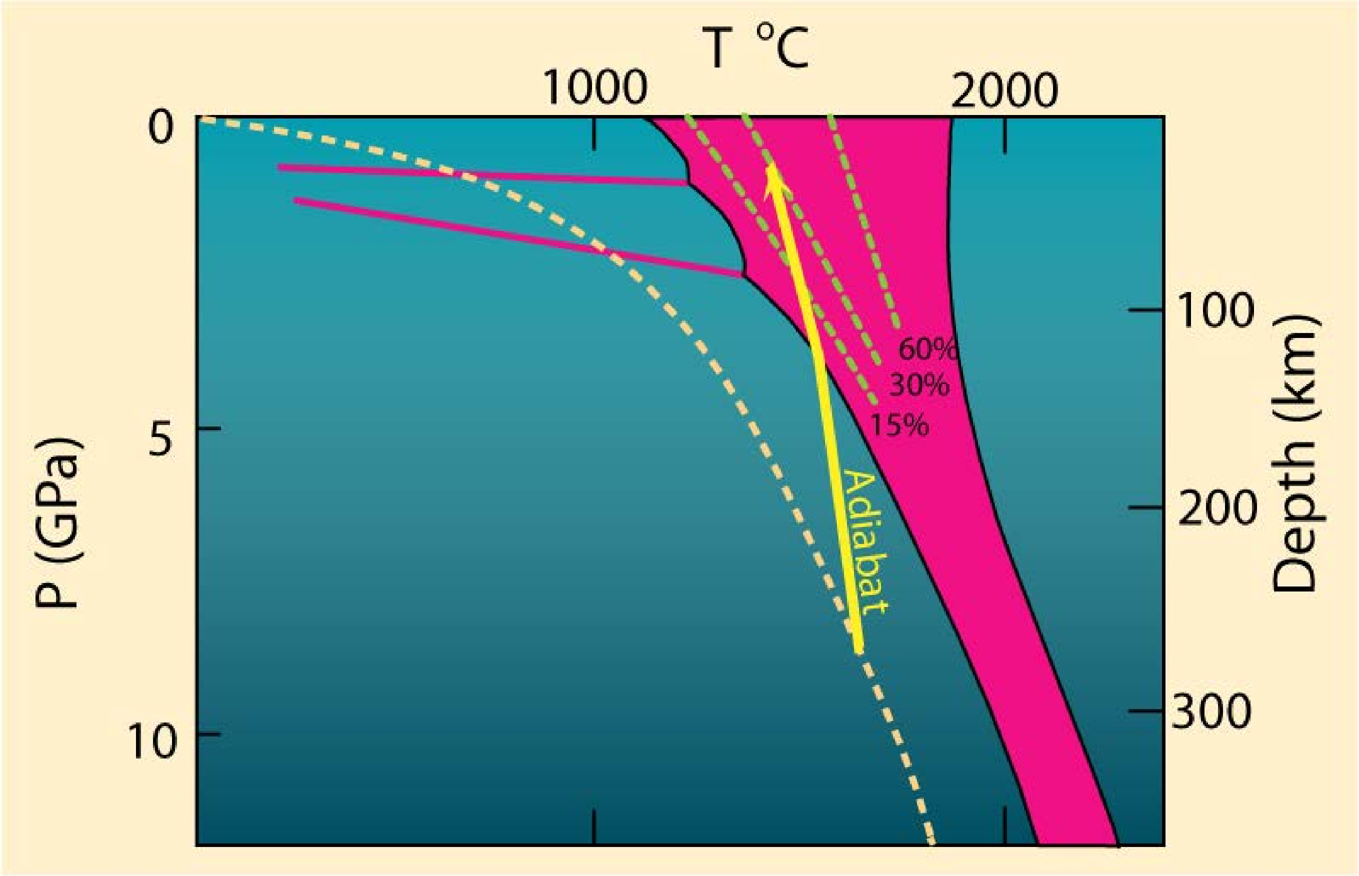

Figure 10.4. Melting by (adiabatic) pressure reduction. Melting begins when the adiabat crosses the solidus and traverses the shaded melting interval. Dashed lines represent approximate % melting.

3) Add volatiles (especially H_2O)

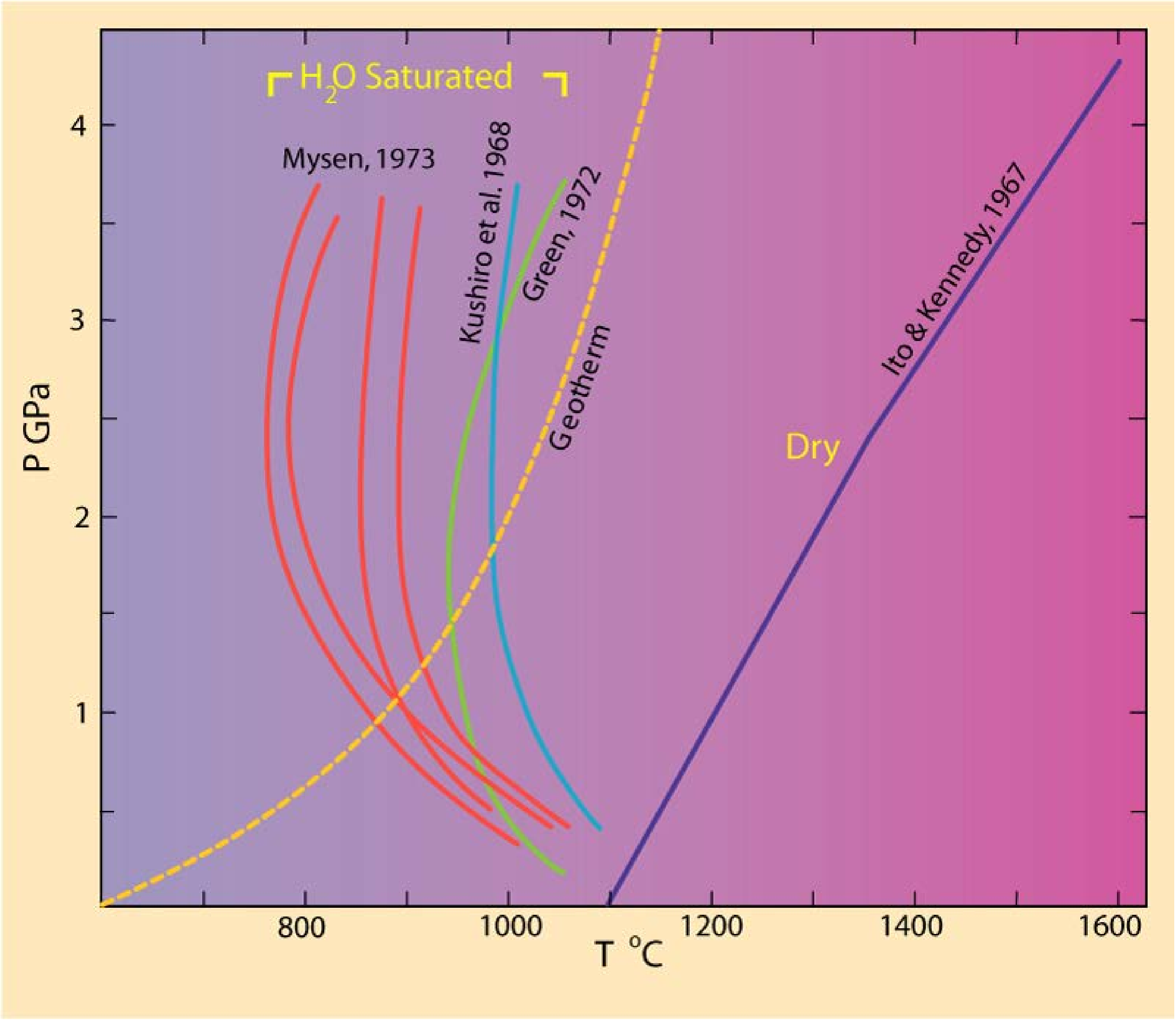

Figure 10.4. Dry peridotite solidus compared to several experiments on H2O-saturated peridotites.

Fraction melted is limited by the availability of water

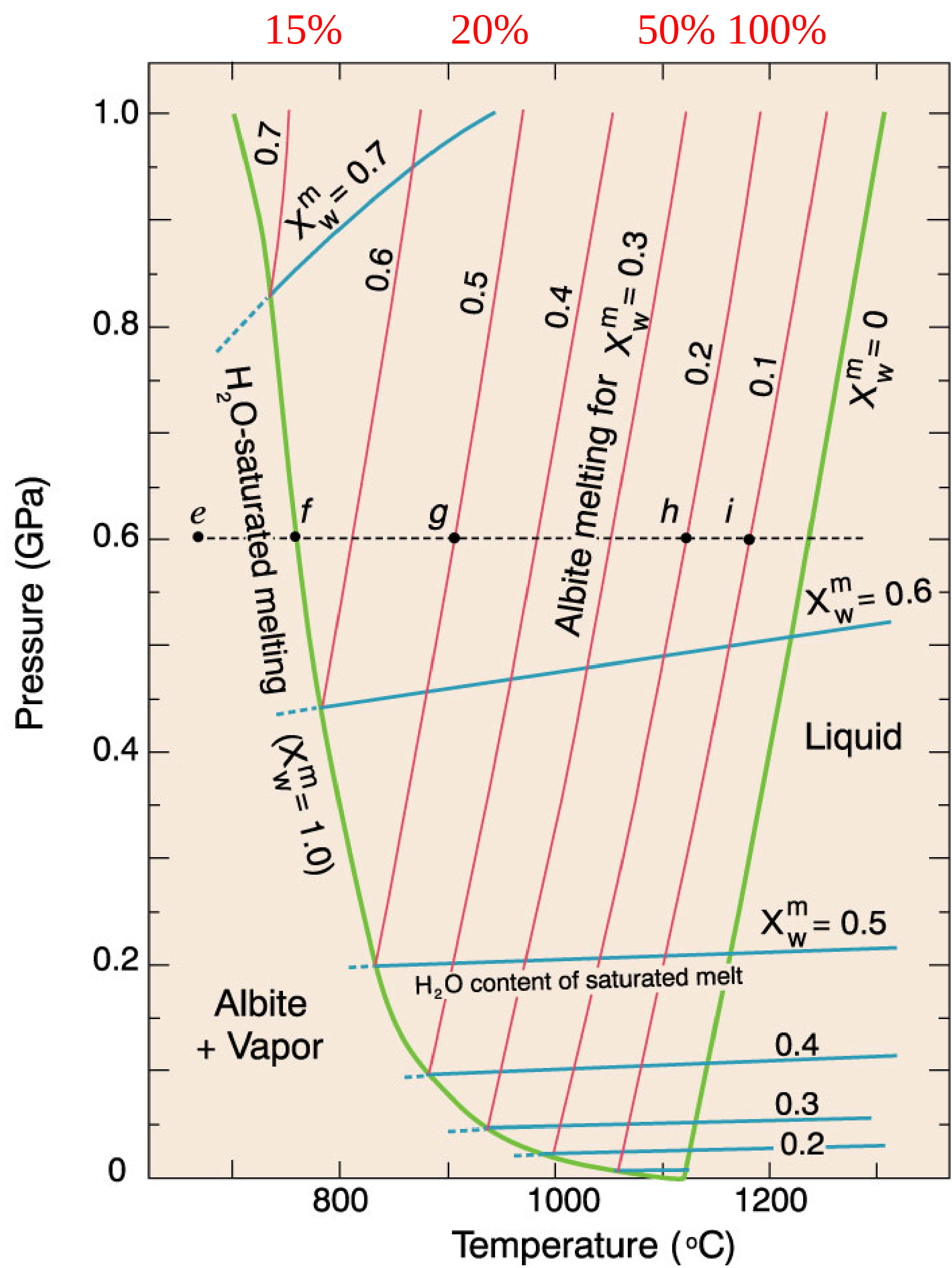

Figure 7.22. Pressure-temperature projection of the melting relationships in the system albite-H_2O. From Burnham and Davis (1974). A J Sci., 274, 902-940.

- Heating of amphibole-bearing peridotite
  1) Ocean geotherm
  2) Shield geotherm

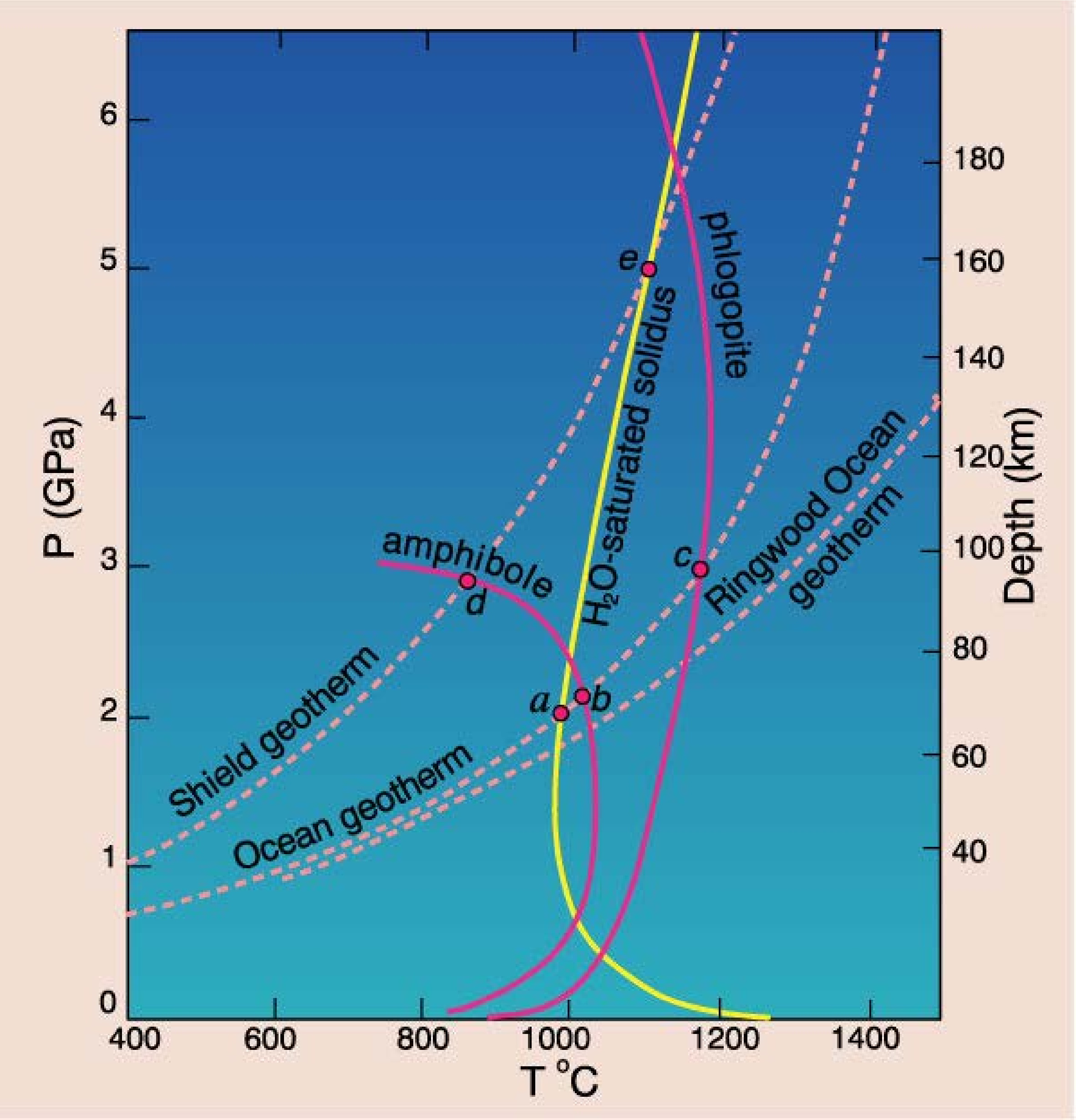

Figure 10.6 Phase diagram (partly schematic) for a hydrous mantle system, including the H2O-saturated lherzolite solidus of Kushiro et al. (1968), the dehydration breakdown curves for amphibole (Millhollen et al., 1974) and phlogopite (Modreski and Boettcher, 1973), plus the ocean and shield geotherms of Clark and Ringwood (1964) and Ringwood (1966). After Wyllie (1979). In H. S. Yoder (ed.), *The Evolution of the Igneous Rocks. Fiftieth Anniversary Perspectives.* Princeton University Press, Princeton, N. J, pp. 483-520.

Melts can be created under realistic circumstances

- Plates separate and mantle rises at mid-ocean ridges
  - Adiabatic rise → decompression melting
- Hot spots → localized plumes of melt
- Fluid fluxing may give LVL
  - Also important in subduction zones and other settings

Generation of tholeiitic and alkaline basalts from a *chemically* uniform mantle

Variables (other than X)

- Temperature
- Pressure

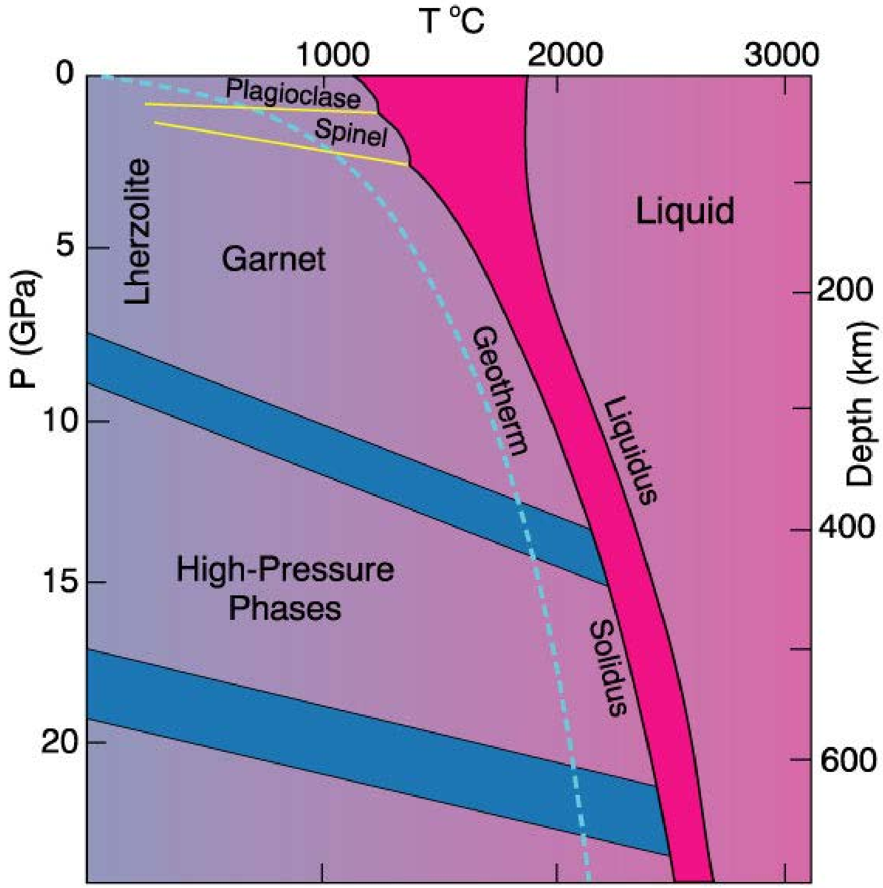

Figure 10.2 Phase diagram of aluminous lherzolite with melting interval (gray), sub-solidus reactions, and geothermal gradient. After Wyllie, P. J. (1981). Geol. Rundsch. 70, 128-153.

Pressure effects:

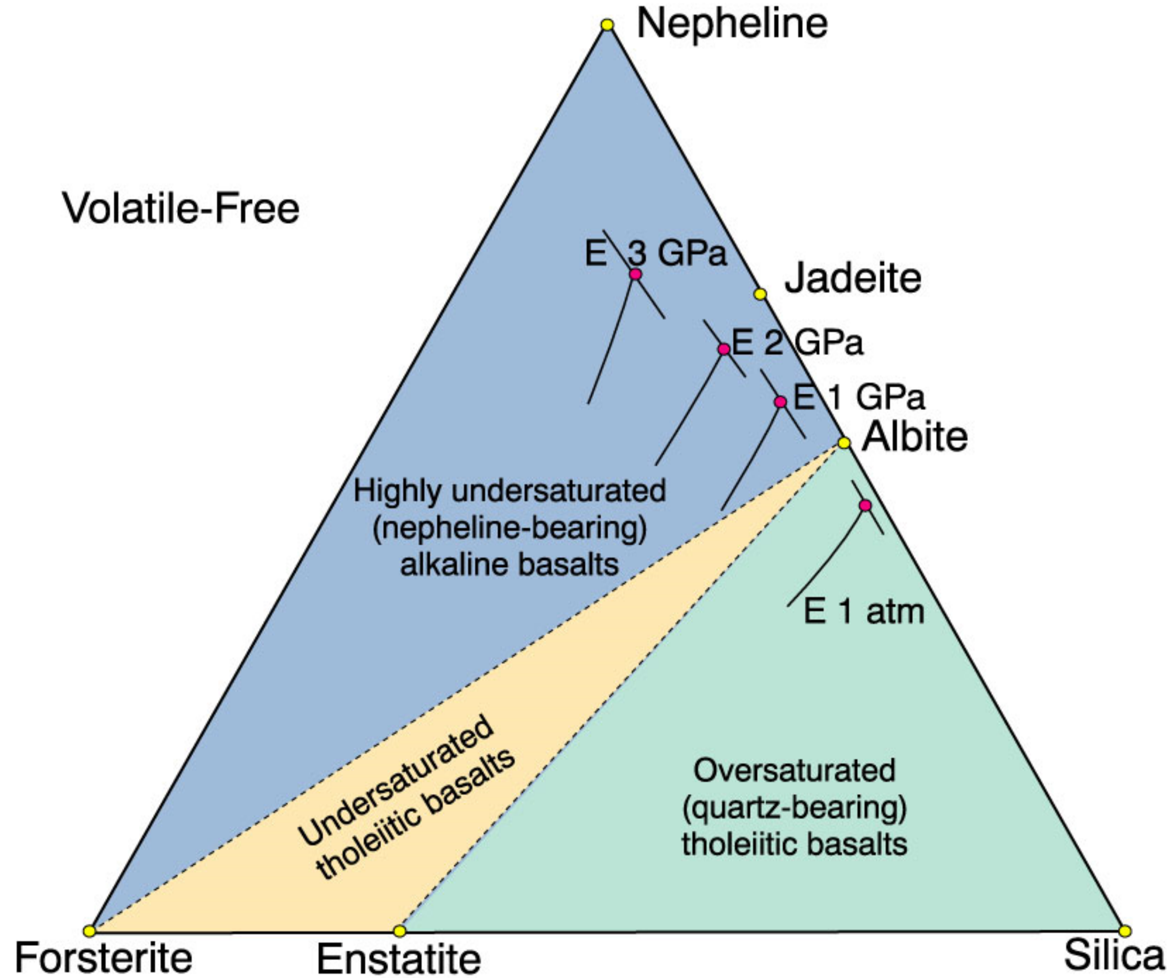

Figure 10.8 Change in the eutectic (first melt) composition with increasing pressure from 1 to 3 GPa projected onto the base of the basalt tetrahedron. After Kushiro (1968), J. Geophys. Res., 73, 619-634.

Liquids and residuum of melted pyrolite

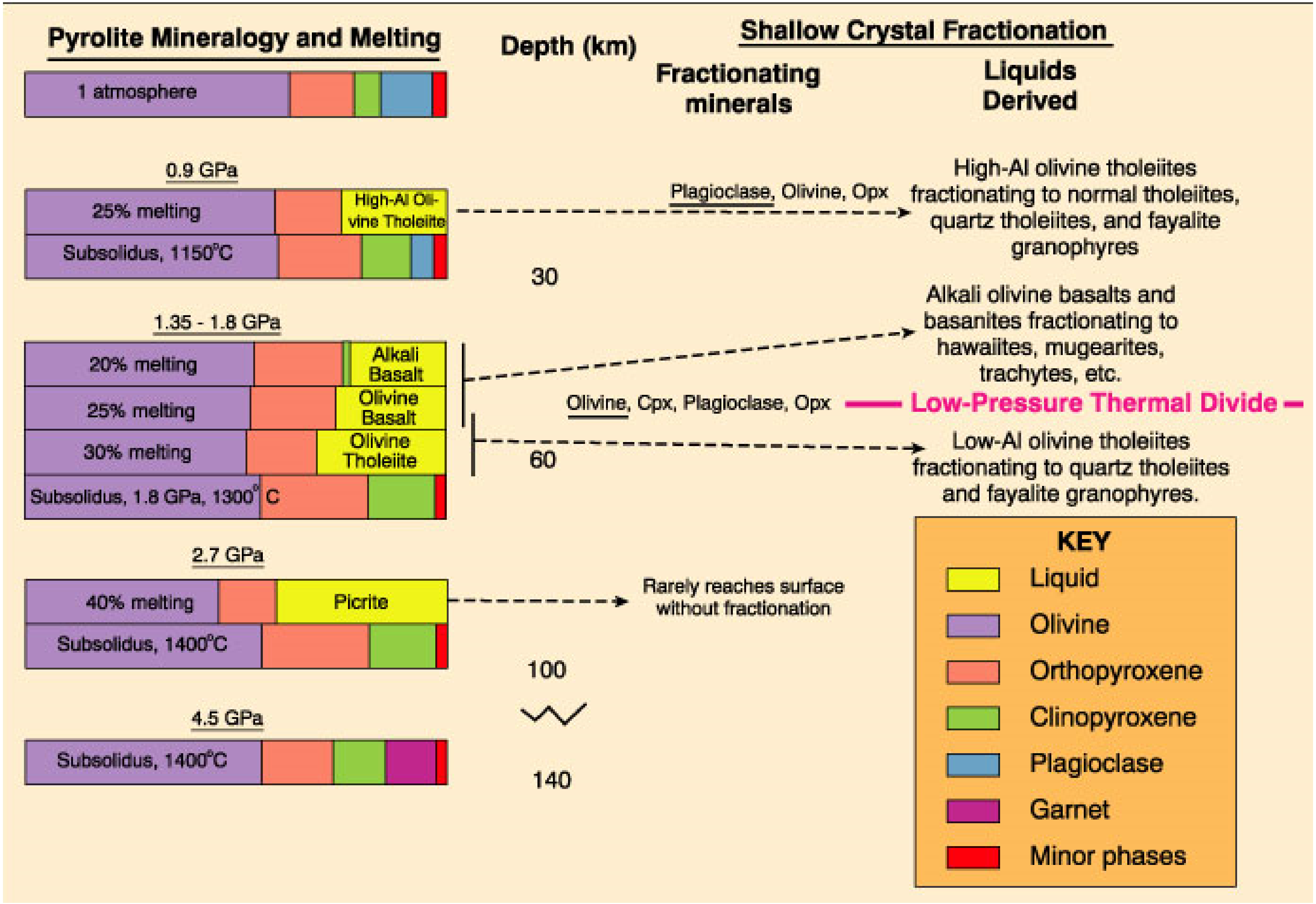

Figure 10.9 After Green and Ringwood (1967). *Earth Planet. Sci. Lett.* 2, 151-160.

Initial Conclusions:

- Tholeiites favored by shallower melting
  - 25% melting at <30 km → tholeiite
  - 25% melting at 60 km → olivine basalt
- Tholeiites favored by greater % partial melting (F)
  - 20 % melting at 60 km → alkaline basalt
    - incompatibles (alkalis) → initial melts
  - 30 % melting at 60 km → tholeiite

Crystal Fractionation of magmas as they rise

- Tholeiite → alkaline by FX at med to high P
- Not at low P
  - Thermal divide
- Al in pyroxenes at Hi P
  - Low-P FX → hi-Al shallow magmas ("hi-Al" basalt)

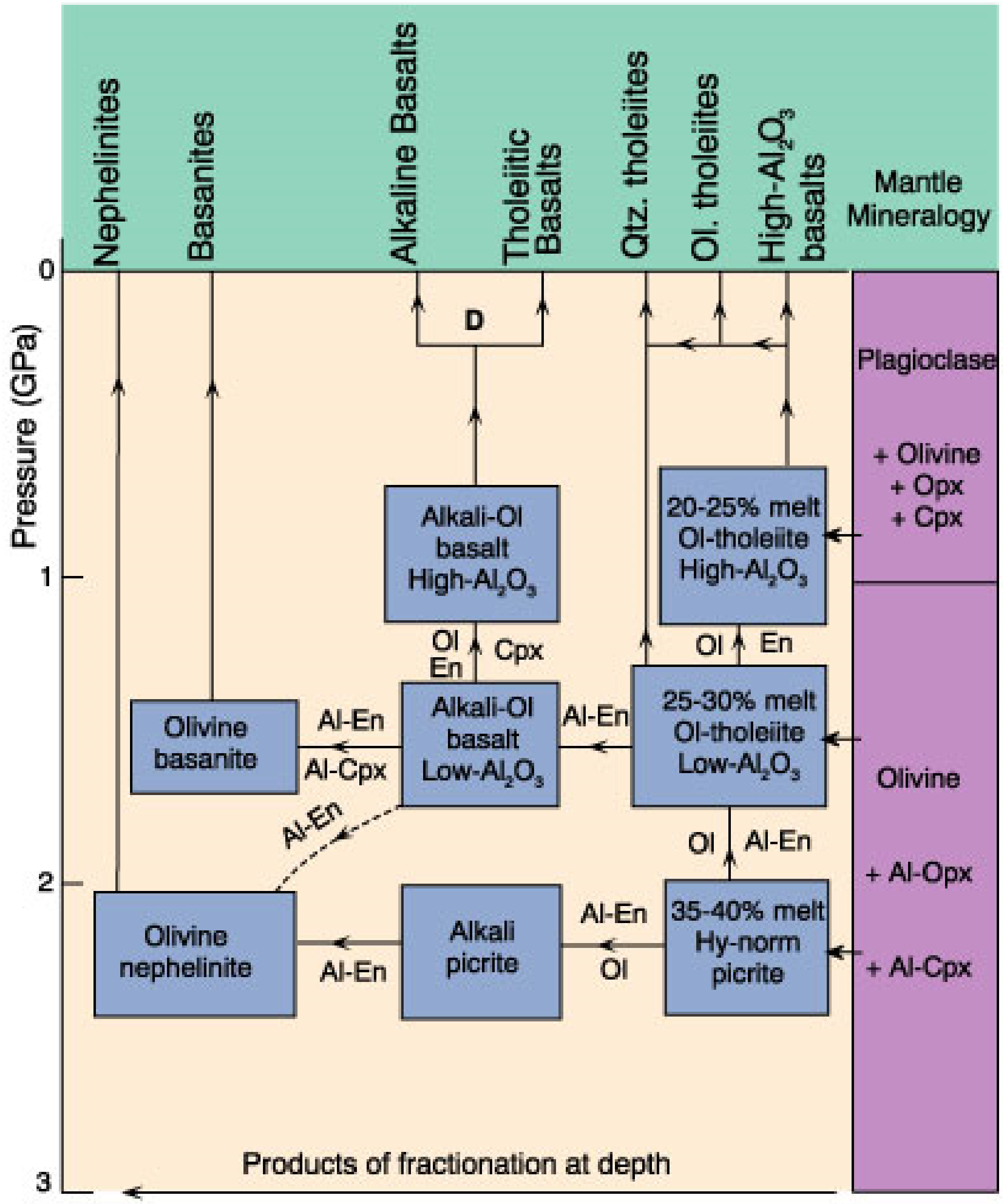

Figure 10.10 Schematic representation of the fractional crystallization scheme of Green and Ringwood (1967) and Green (1969). After Wyllie (1971). *The Dynamic Earth: Textbook in Geosciences*. John Wiley & Sons.

Other, more recent experiments on melting of fertile (initially garnet-bearing) lherzolite confirm that alkaline basalts are favored by high P and low F

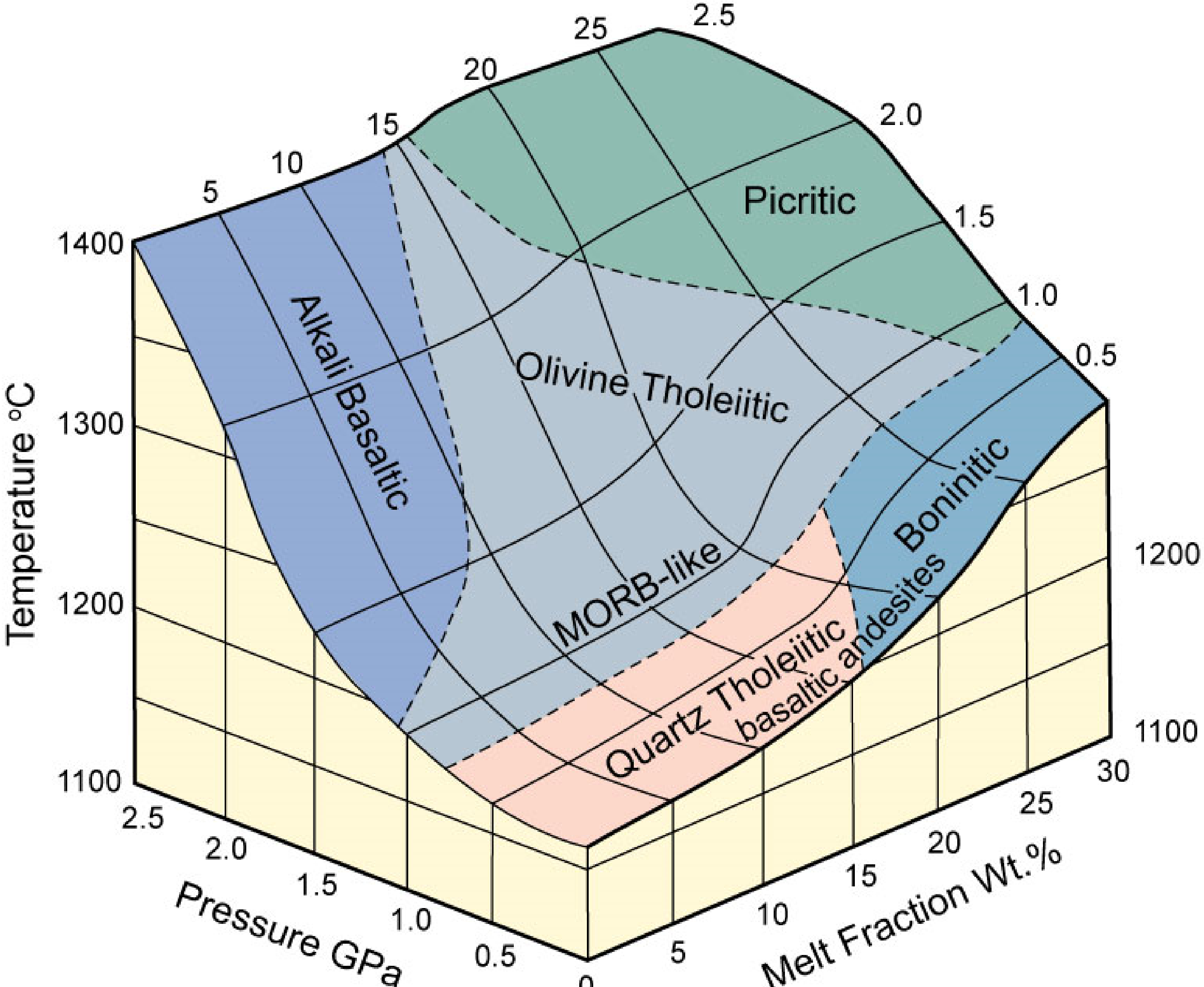

Figure 10.11 After Kushiro (2001).

Primary magmas

- Formed at depth and not subsequently modified by FX or Assimilation
- Criteria
  - Highest Mg# (100Mg/(Mg+Fe)) really → parental magma
  - Experimental results of lherzolite melts
    - Mg# = 66-75
    - Cr > 1000 ppm
    - Ni > 400-500 ppm
    - Multiply saturated

Multiple saturation

- Low P
  - Ol then Plag then Cpx as cool
  - ~70^{o}C T range

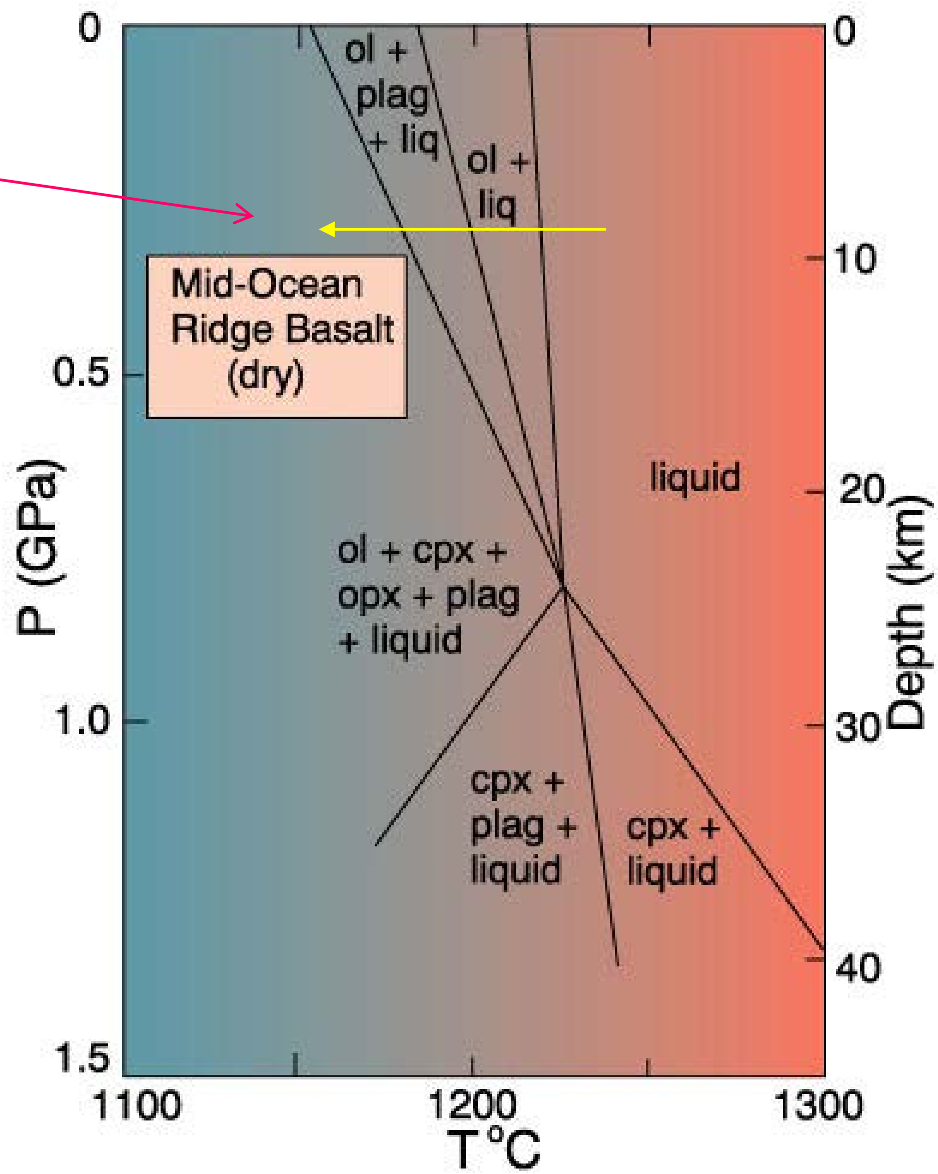

Figure 10.13 Anhydrous P-T phase relationships for a mid-ocean ridge basalt suspected of being a primary magma. After Fujii and Kushiro (1977). *Carnegie Inst. Wash. Yearb.*, 76, 461-465.

Multiple saturation

- Low P
  - Ol then Plag then Cpx as cool
  - 70^{o}C T range
- High P
  - Cpx then Plag then Ol

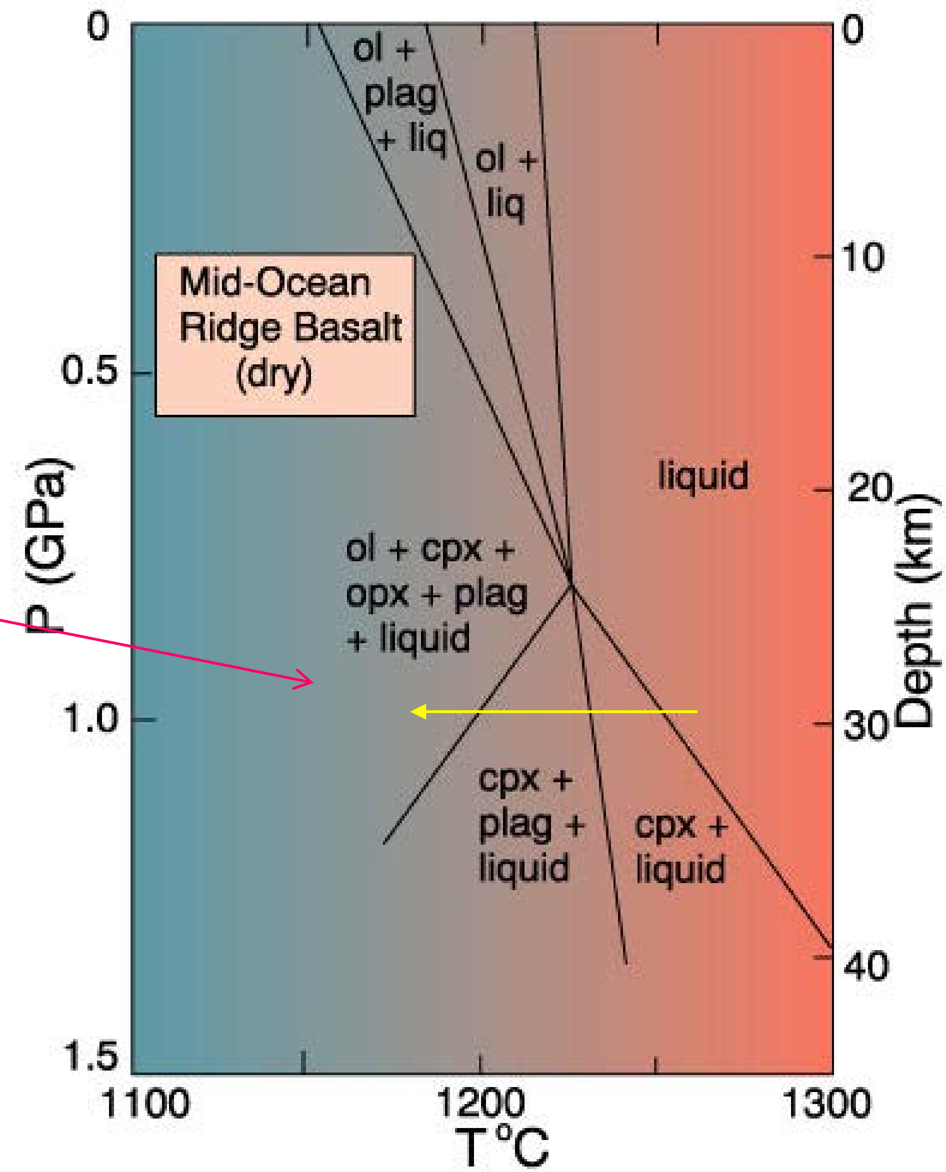

Figure 10.13 Anhydrous P-T phase relationships for a mid-ocean ridge basalt suspected of being a primary magma. After Fujii and Kushiro (1977). *Carnegie Inst. Wash. Yearb.*, 76, 461-465.

Multiple saturation

- Low P
  - Ol then Plag then Cpx as cool
  - 70^{o}C T range
- High P
  - Cpx then Plag then Ol
- 25 km get all at once
  - = Multiple saturation
  - Suggests that 25 km is the depth of last eq^{m} with the mantle

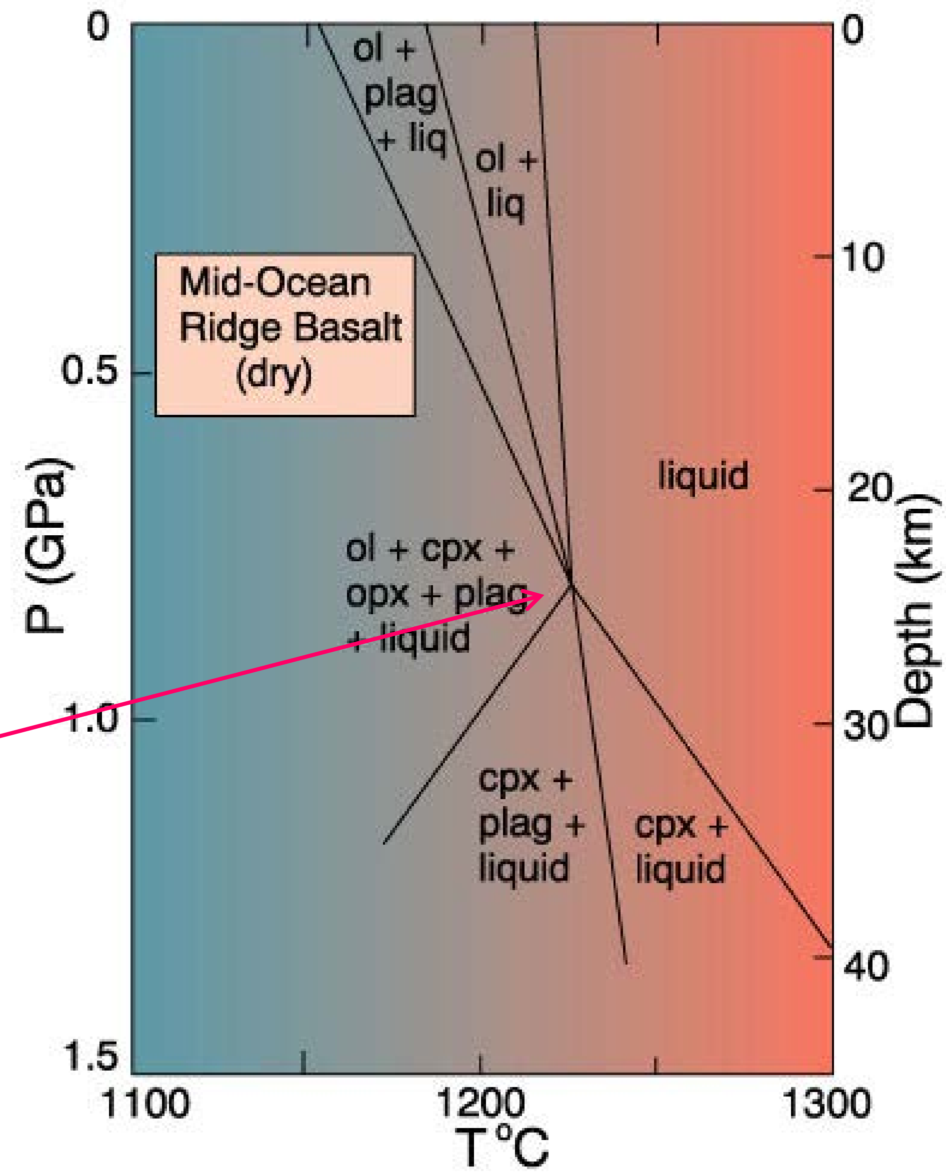

Summary

- A chemically homogeneous mantle can yield a variety of basalt types
- Alkaline basalts are favored over tholeiites by deeper melting and by low % PM
- Fractionation at moderate to high depths can also create alkaline basalts from tholeiites
- At low P there is a thermal divide that separates the two series

Review of REE

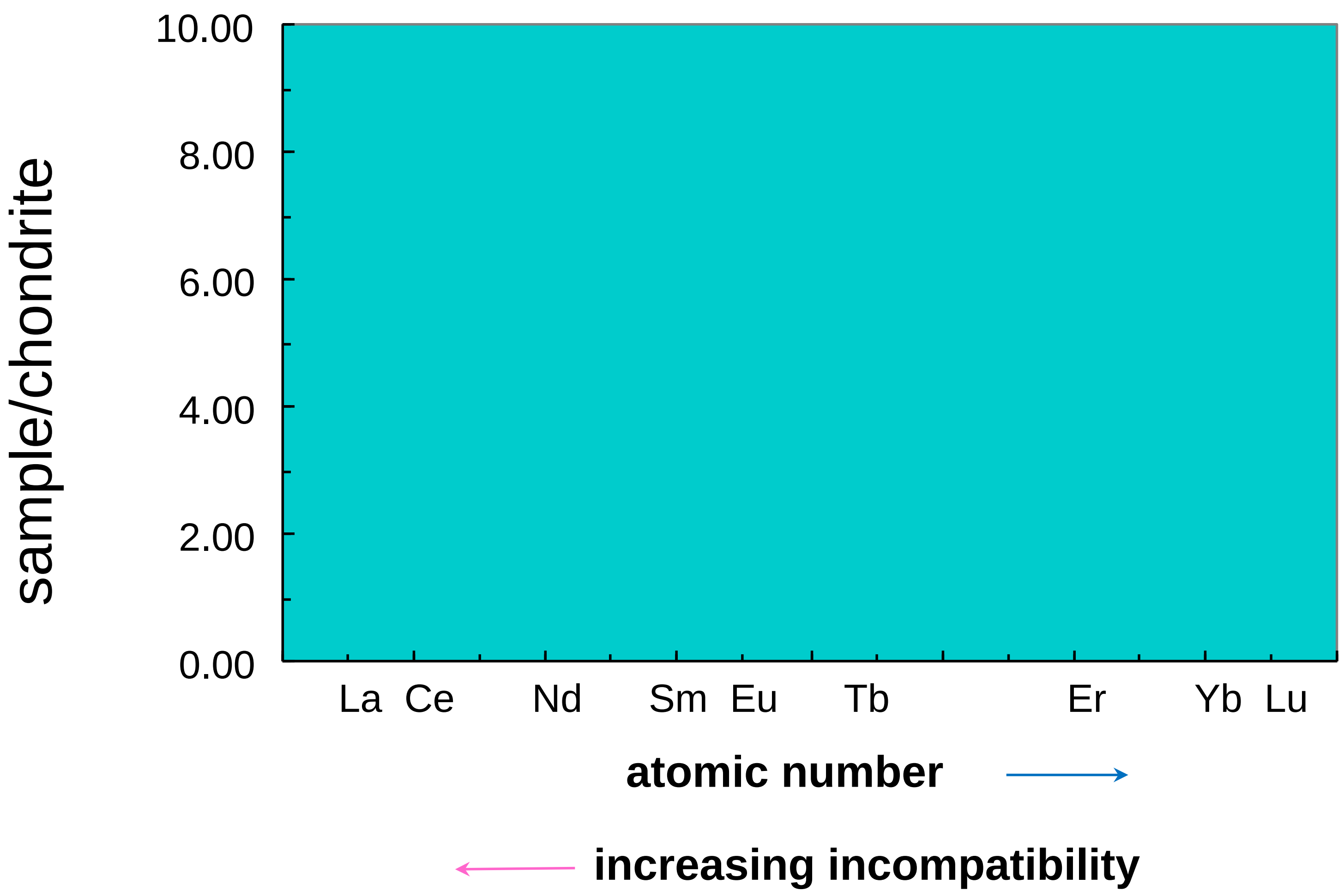

Review of REE

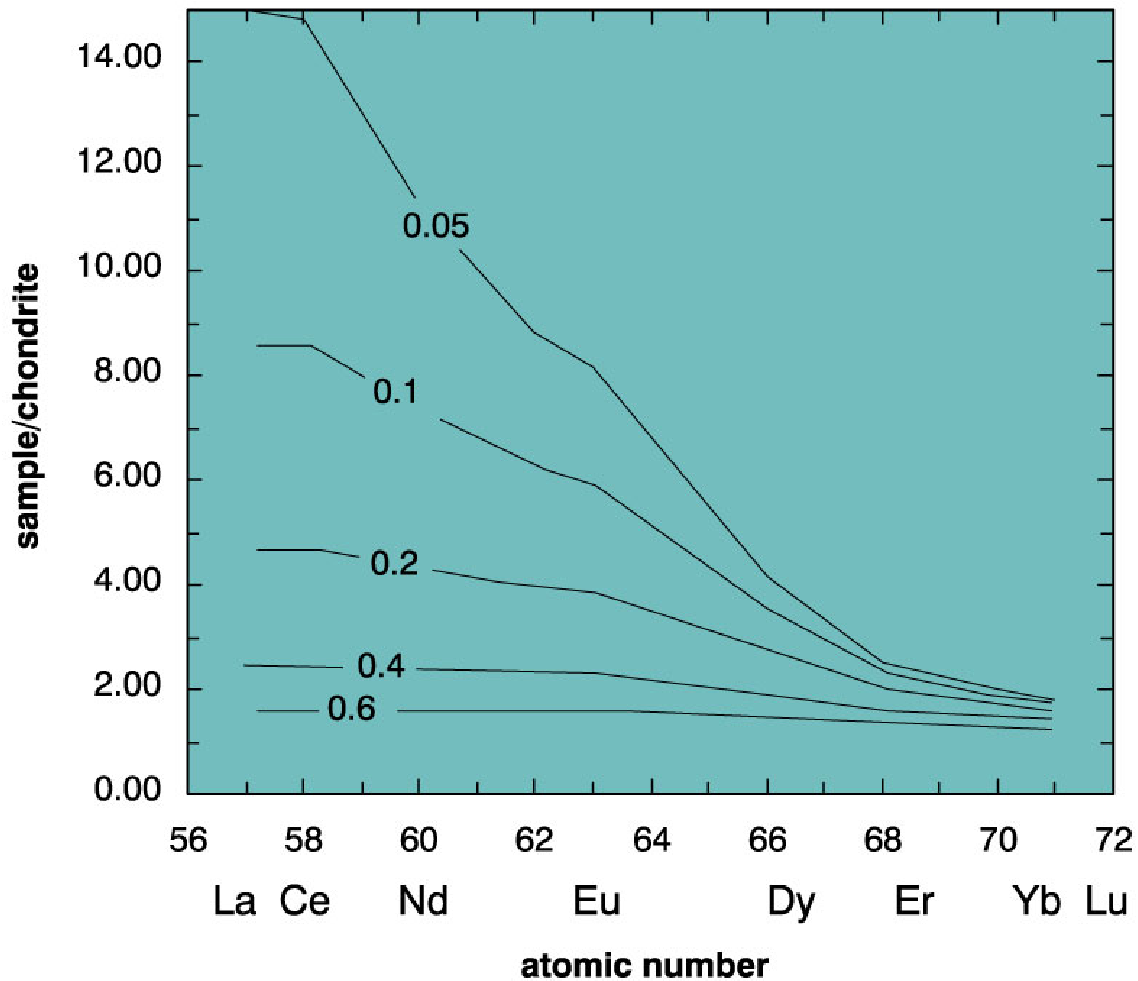

Figure 9.4. Rare Earth concentrations (normalized to chondrite) for melts produced at various values of F via melting of a hypothetical garnet lherzolite using the batch melting model (equation 9-5). From Winter (2001) An Introduction to Igneous and Metamorphic Petrology. Prentice Hall.

← **increasing incompatibility**

REE data for oceanic basalts

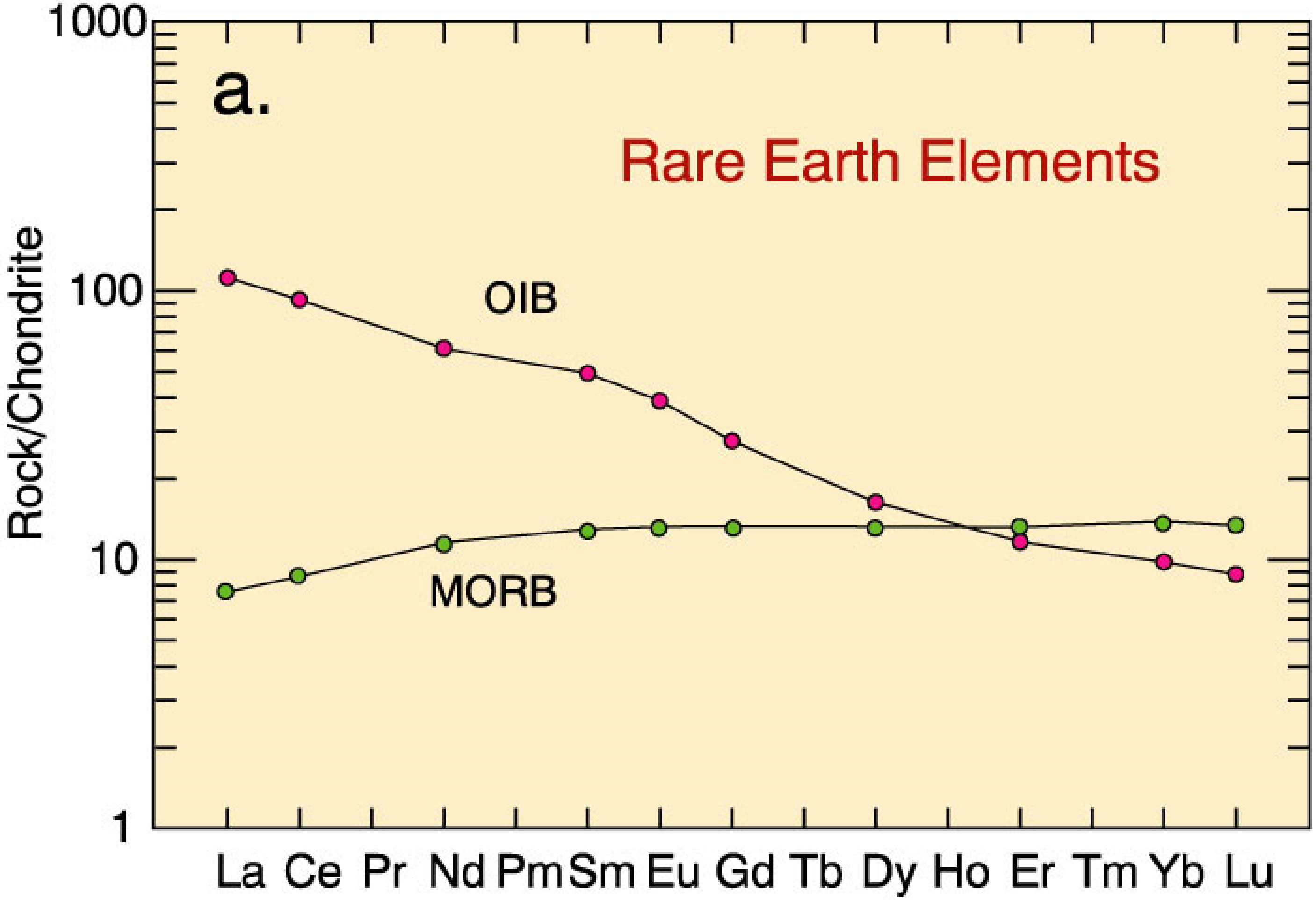

increasing incompatibility

Figure 10.14a. REE diagram for a typical alkaline ocean island basalt (OIB) and tholeiitic mid-ocean ridge basalt (MORB). From Winter (2001) An Introduction to Igneous and Metamorphic Petrology. Prentice Hall. Data from Sun and McDonough (1989).

Spider diagram for oceanic basalts

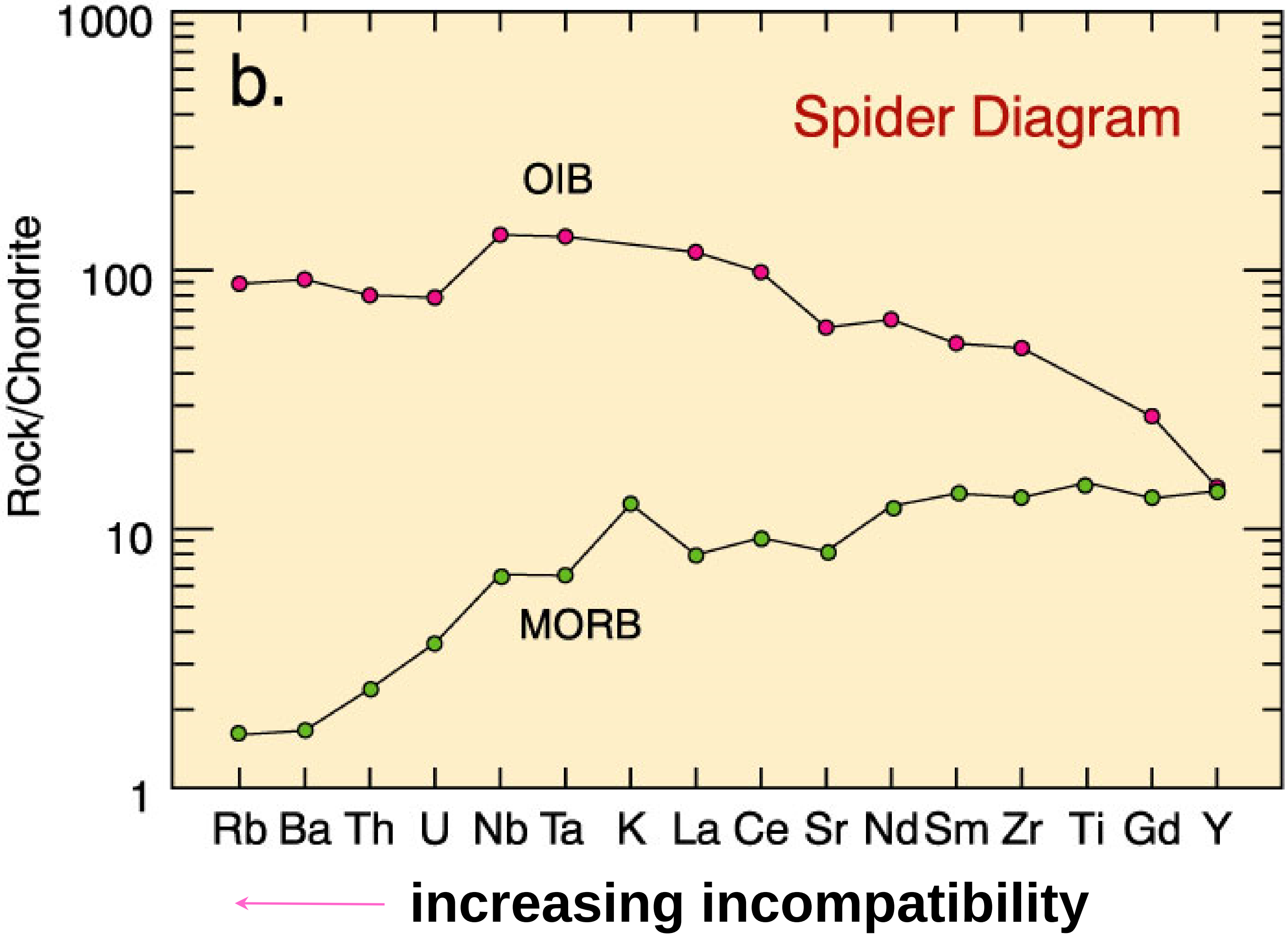

Figure 10.14b. Spider diagram for a typical alkaline ocean island basalt (OIB) and tholeiitic mid-ocean ridge basalt (MORB). From Winter (2001) An Introduction to Igneous and Metamorphic Petrology. Prentice Hall. Data from Sun and McDonough (1989).

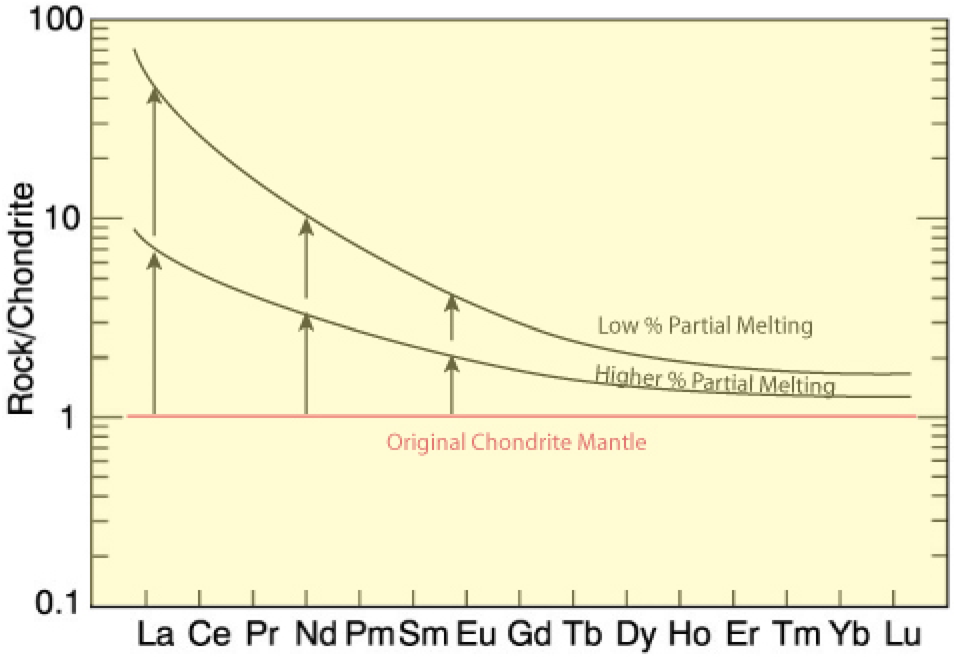

Suggests different mantle source types, but isn’t conclusive.

Depleted mantle could → both MORB and OIB.

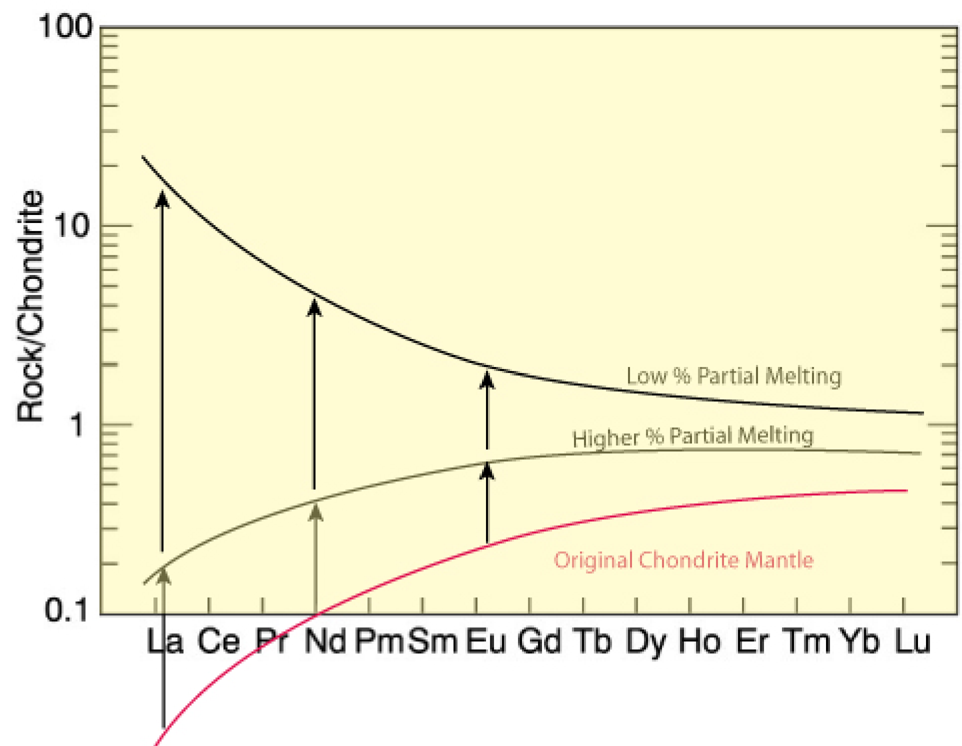

REE data for UM xenoliths

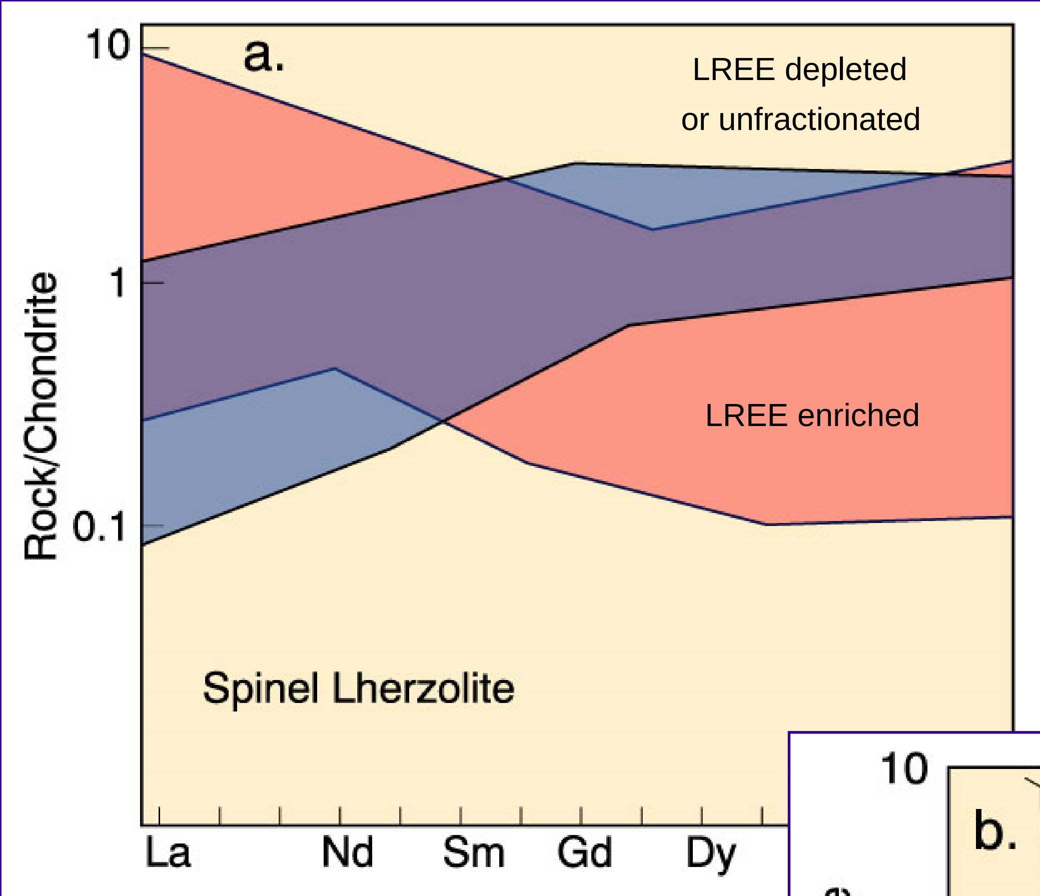

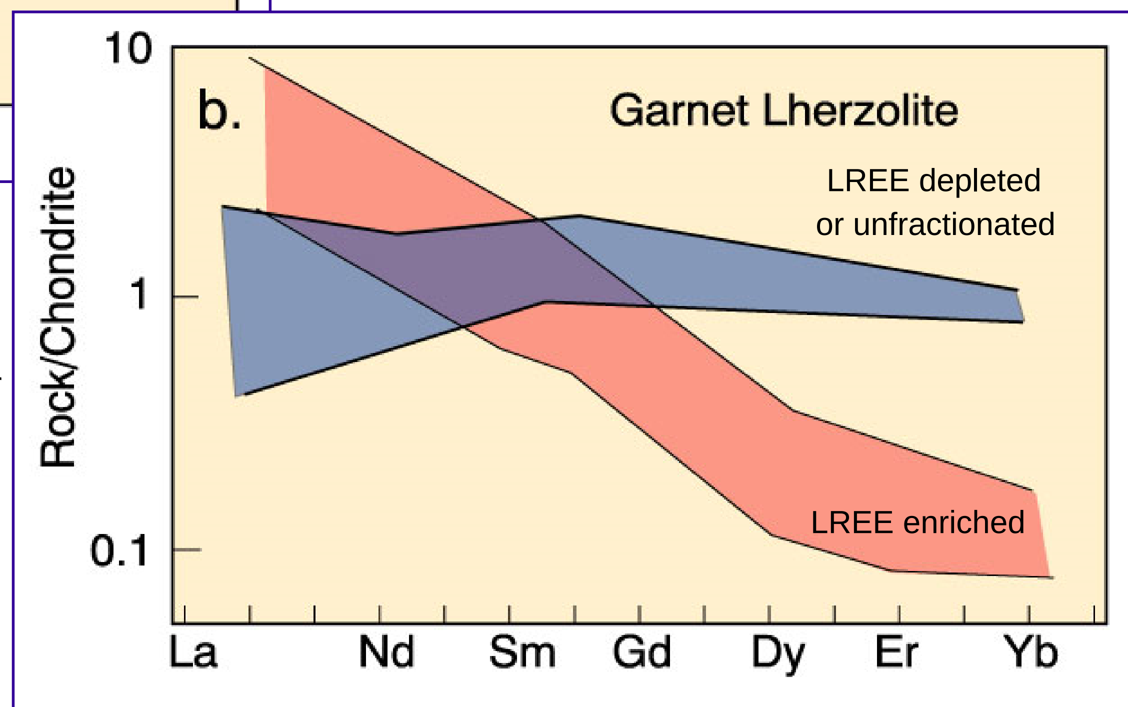

Figure 10.15 Chondrite-normalized REE diagrams for spinel (a) and garnet (b) lherzolites. After Basaltic Volcanism Study Project (1981). Lunar and Planetary Institute.

Review of Sr isotopes

- $^{87}Rb \rightarrow {}^{87}Sr \quad \lambda = 1.42 \times 10^{-11}$ a
- Rb (parent) conc. in enriched reservoir (incompatible)
- Enriched reservoir

  develops more

  ^{87}Sr over time
- Depleted reservoir

  (less Rb)

  develops less

  ^{87}Sr over time

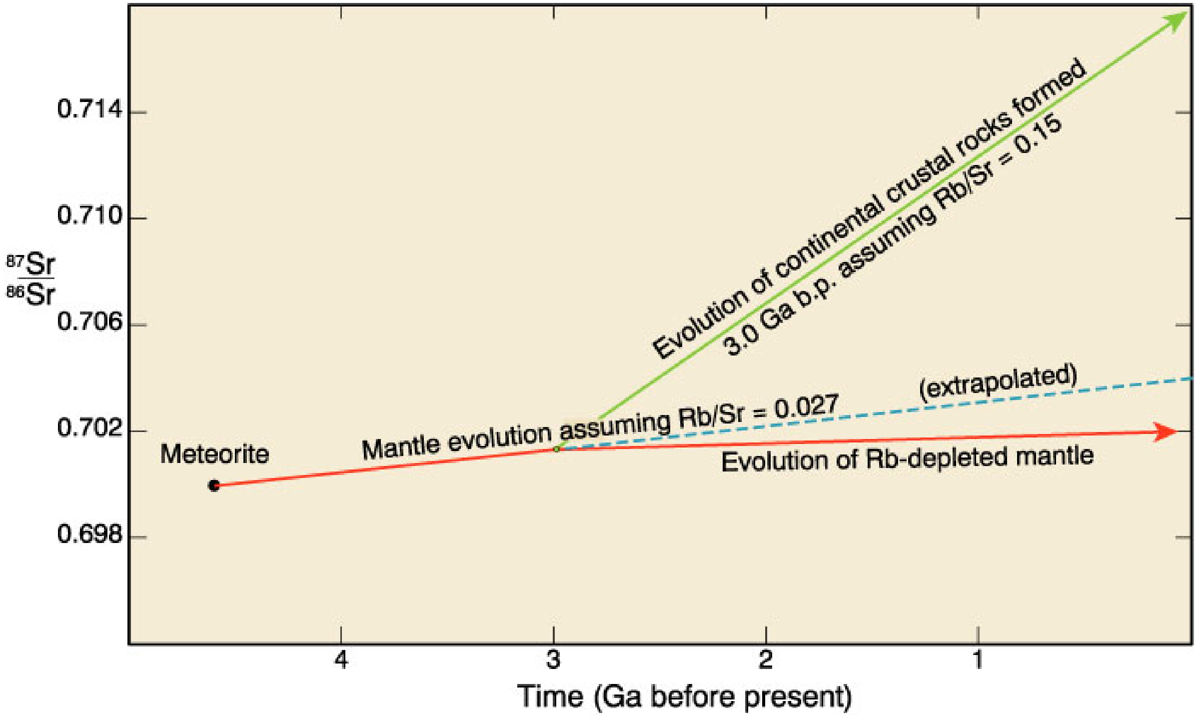

Figure 9.13. After Wilson (1989). Igneous Petrogenesis. Unwin Hyman/Kluwer.

Review of Nd isotopes

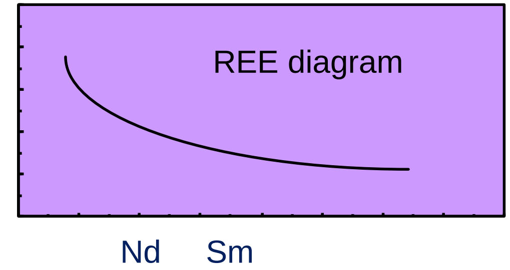

- $^{147}Sm \rightarrow {}^{143}Nd$ $\lambda = 6.54 \times 10^{-13}$ a
- Nd (daughter) → enriched reservoir > Sm
- Enriched reservoir develops ***less*** ^{143}Nd over time
- Depleted res. (higher Sm/Nd) develops ***higher*** $^{143}Nd/^{144}Nd$ over time

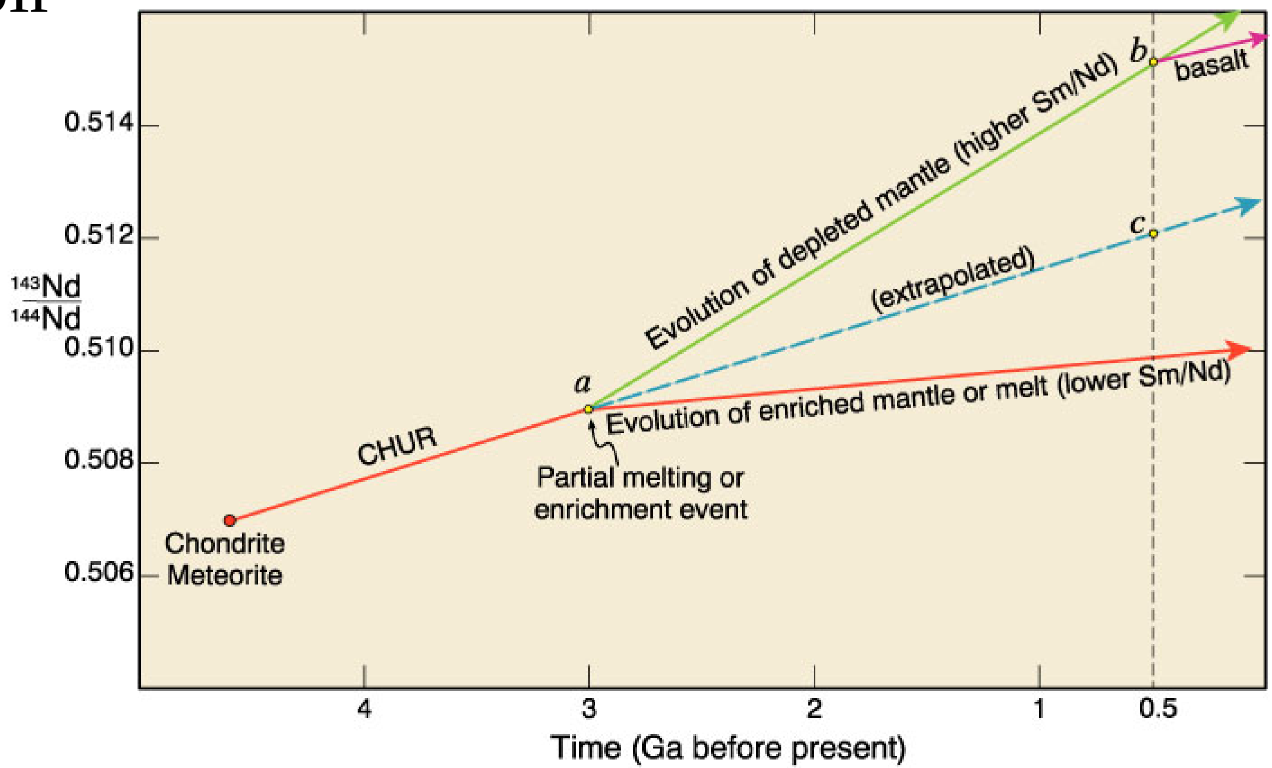

Figure 9.15. After Wilson (1989). Igneous Petrogenesis. Unwin Hyman/Kluwer.

Nd and Sr isotopes of Ocean Basalts
"Mantle Array"

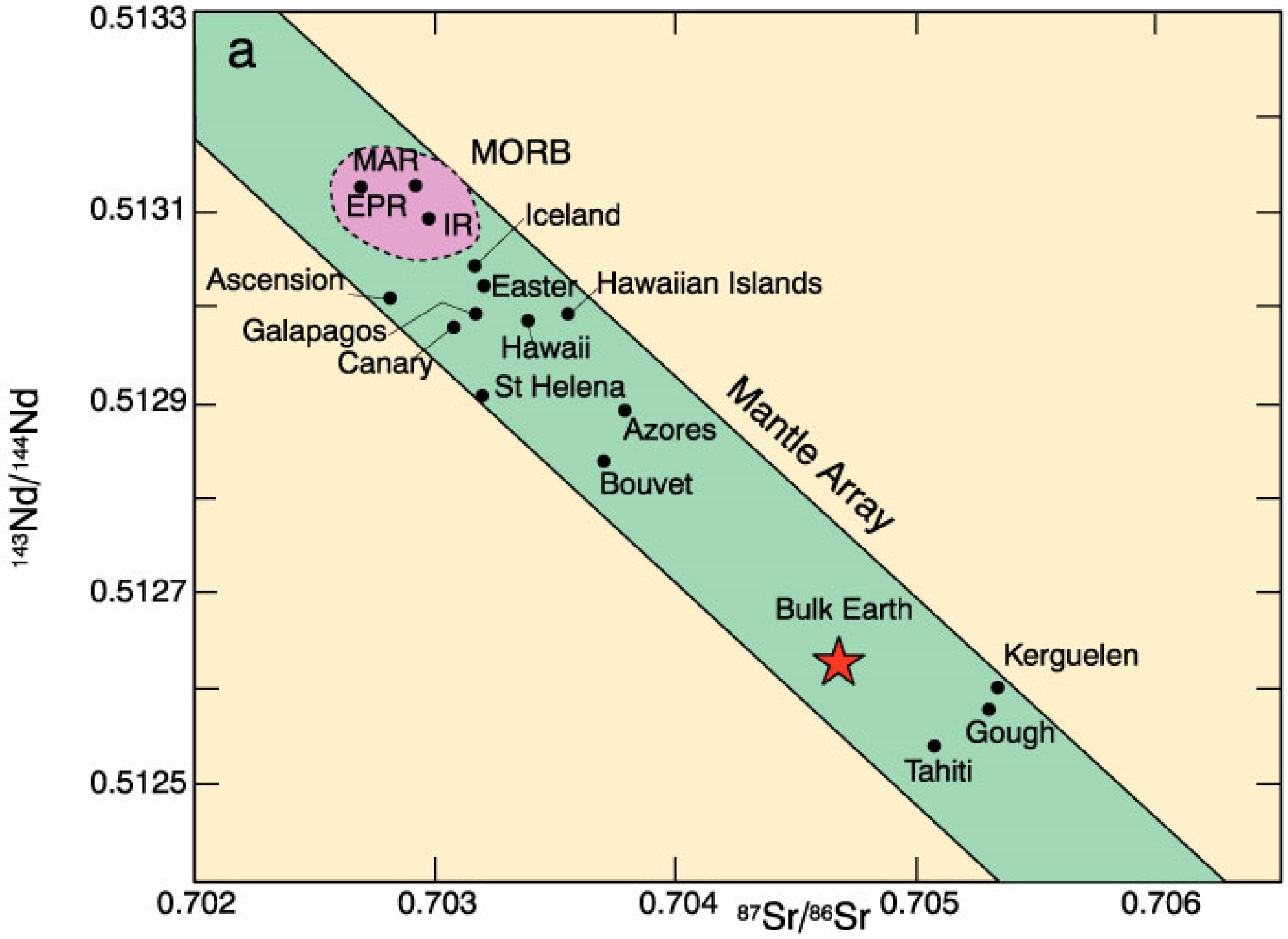

Figure 10.16a. Initial ^{143}Nd/^{144}Nd vs. ^{87}Sr/^{86}Sr for oceanic basalts. From Wilson (1989). Igneous Petrogenesis. Unwin Hyman/Kluwer. Data from Zindler *et al*. (1982) and Menzies (1983).

Nd and Sr isotopes of Kimberlite Xenoliths

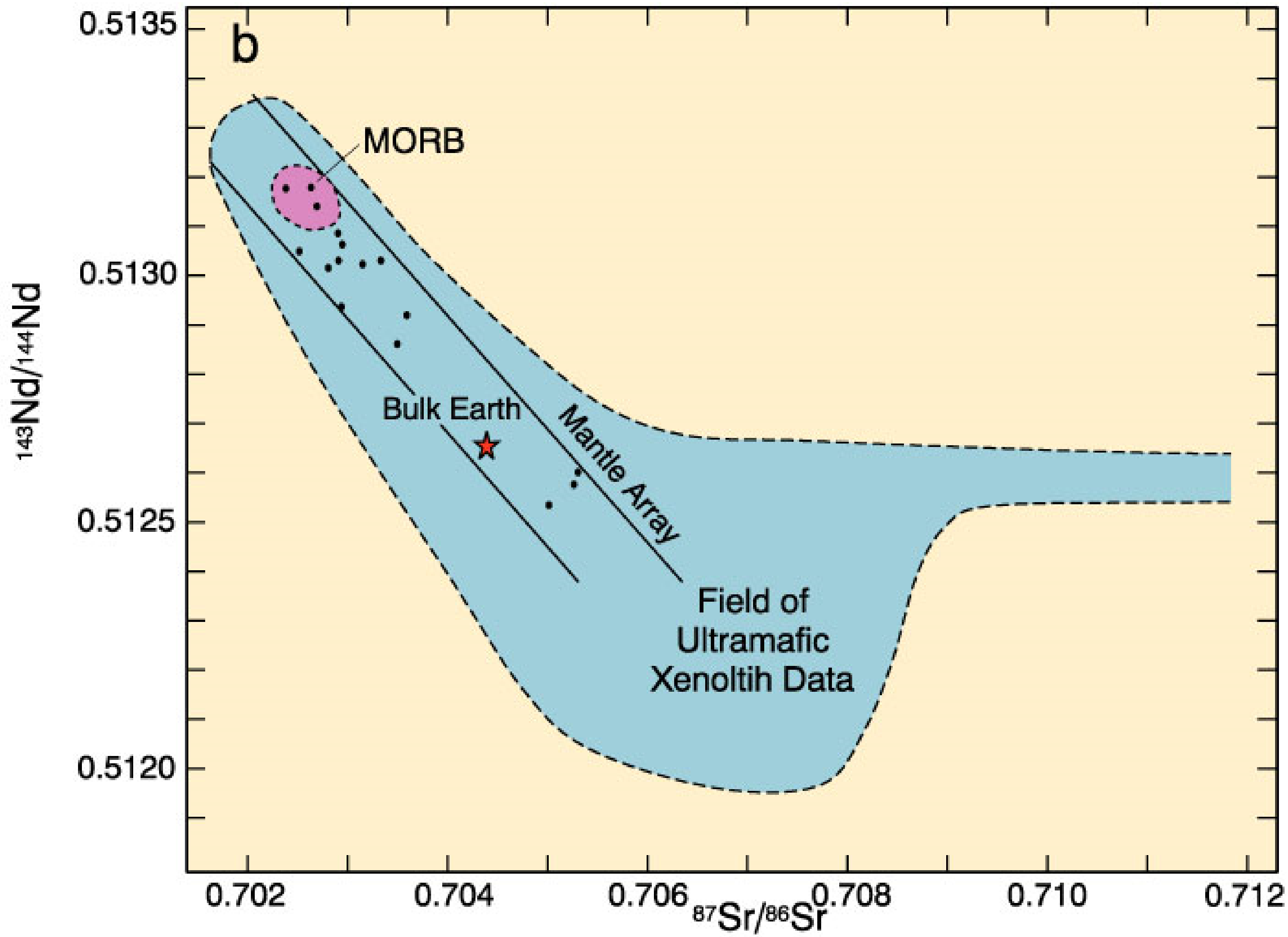

Figure 10.16b. Initial $^{143}Nd/^{144}Nd$ vs. $^{87}Sr/^{86}Sr$ for mantle xenoliths. From Wilson (1989). Igneous Petrogenesis. Unwin Hyman/Kluwer. Data from Zindler *et al*. (1982) and Menzies (1983).

"Whole Mantle" circulation model

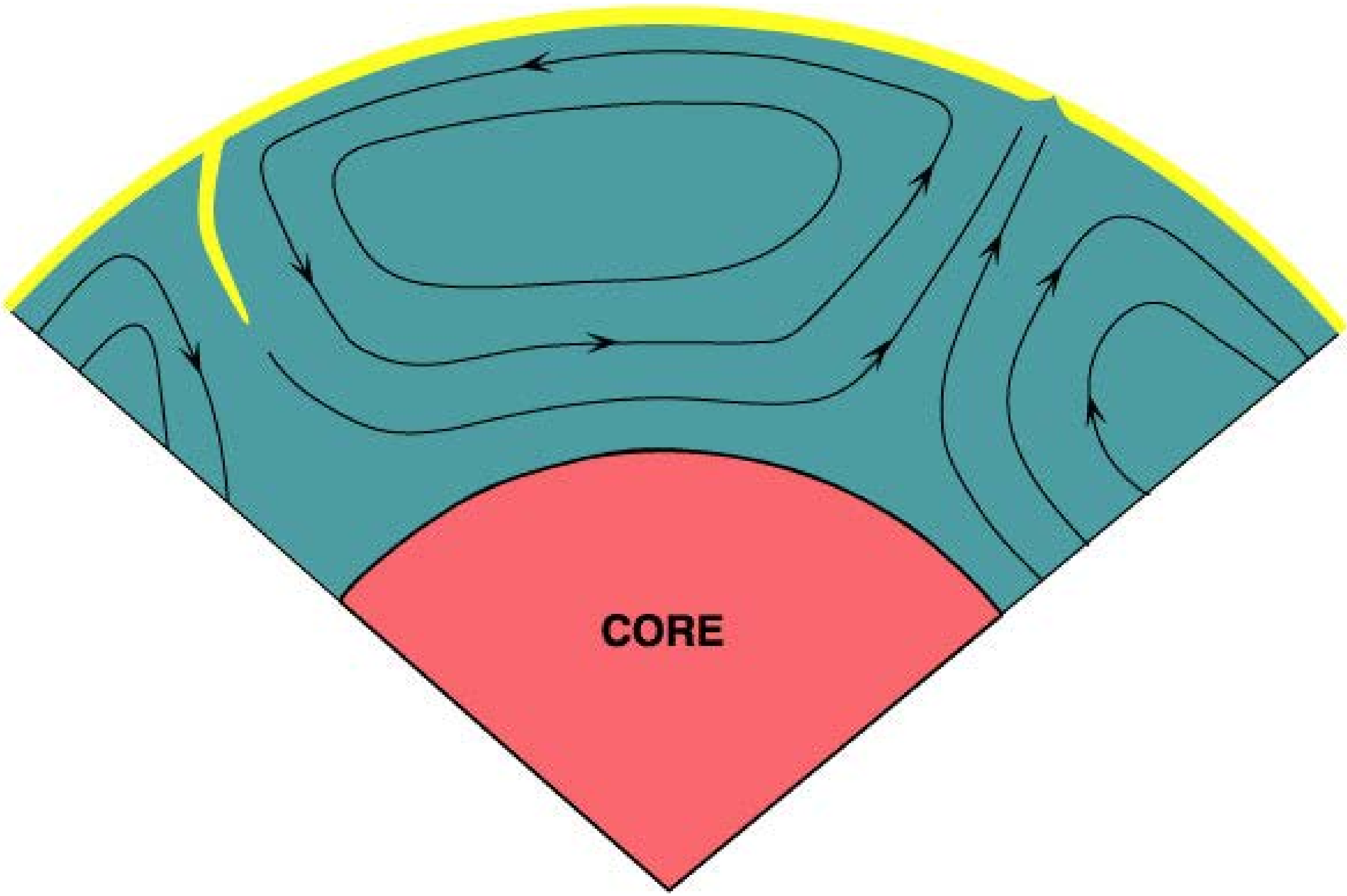

Figure 10-17a After Basaltic Volcanism Study Project (1981). Lunar and Planetary Institute.

“Two-Layer” circulation model

- Upper depleted mantle = MORB source
- Lower undepleted & enriched OIB source

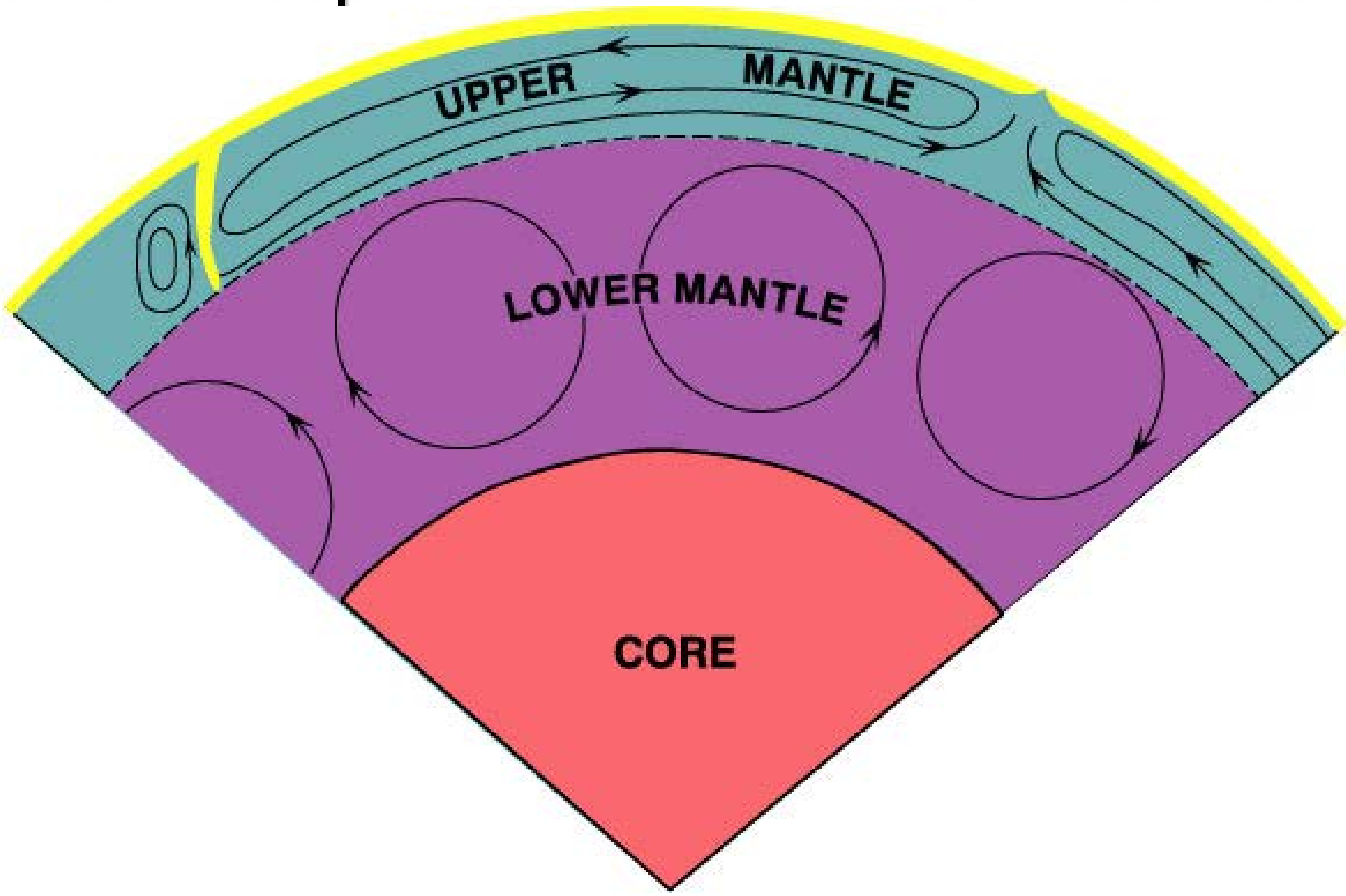

Figure 10-17b After Basaltic Volcanism Study Project (1981). Lunar and Planetary Institute.

Experiments on melting enriched vs. depleted mantle samples:

1. Depleted Mantle
   - Tholeiite easily created by 10-30% PM
   - More silica saturated at lower P
   - Grades toward alkalic at higher P

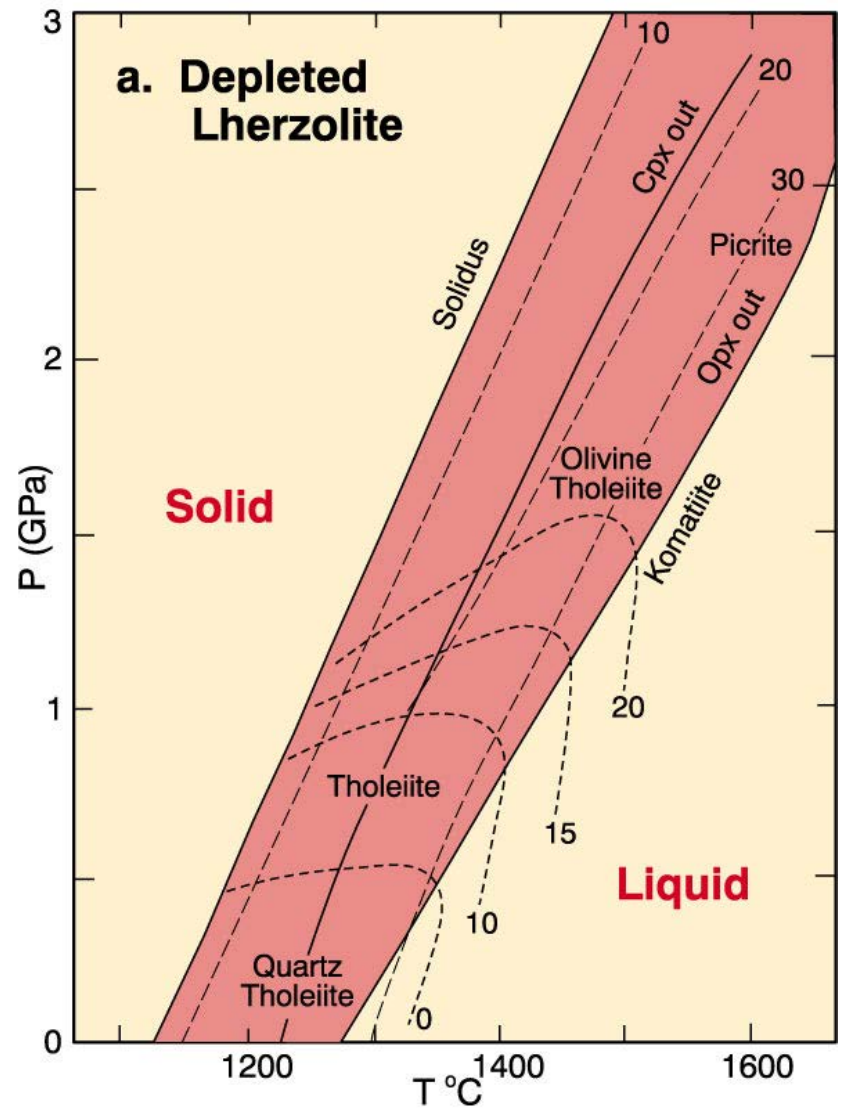

Figure 10-18a. Results of partial melting experiments on depleted lherzolites. Dashed lines are contours representing percent partial melt produced. Strongly curved lines are contours of the normative olivine content of the melt. “Opx out” and “Cpx out” represent the degree of melting at which these phases are completely consumed in the melt. After Jaques and Green (1980). Contrib. Mineral. Petrol., 73, 287-310.

Experiments on melting enriched vs. depleted mantle samples:

2. Enriched Mantle

- Tholeiites extend to higher P than for DM
- Alkaline basalt field at higher P yet
  - ☞ And lower % PM

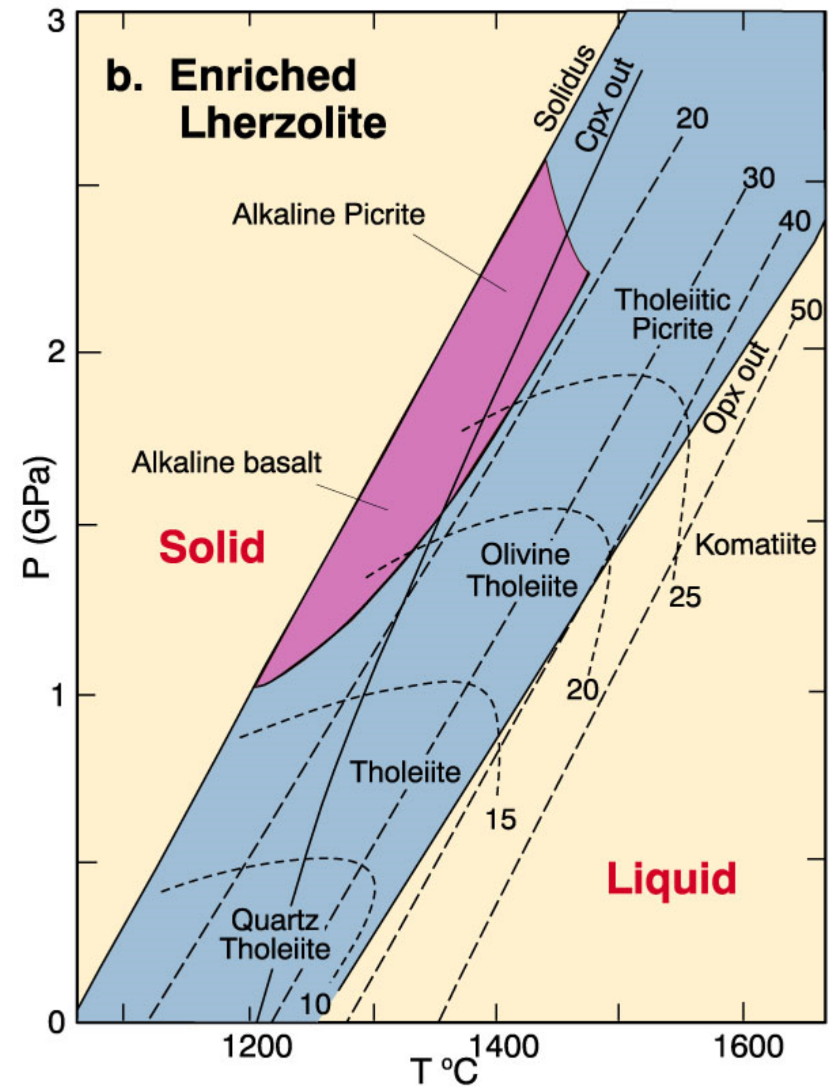

Figure 10-18b. Results of partial melting experiments on fertile lherzolites. Dashed lines are contours representing percent partial melt produced. Strongly curved lines are contours of the normative olivine content of the melt. "Opx out" and "Cpx out" represent the degree of melting at which these phases are completely consumed in the melt. The shaded area represents the conditions required for the generation of alkaline basaltic magmas. After Jaques and Green (1980). Contrib. Mineral. Petrol., 73, 287-310.